Numerical solution of the Black-Scholes equation with a small number of grid points

C.C.W. Leentvaar

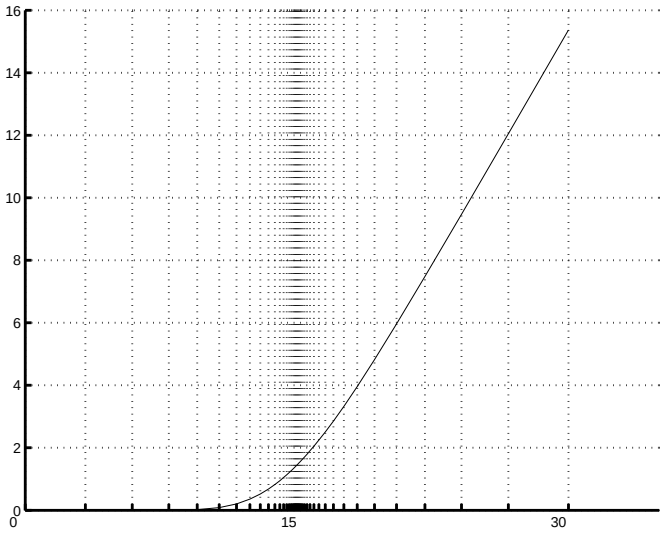

Master's Thesis

Delft University of Technology
Faculty of Electrical Engineering,
Mathematics and Computer Science,
Section Applied Mathematics,
Numerical Analysis Group
Supervisor: Dr. Ir. C.W. Oosterlee

March-December 2003.

Afstudeercommissie:

Prof.dr.ir. P. Wesseling
Dr.ir. J.A.M van der Weide,
Dr.ir. C.W. Oosterlee.

Samenvatting

Opties zijn koop- of verkoopovereenkomsten, die in de toekomst uitgevoerd kunnen worden. De houder van een optie heeft niet de plicht, maar het recht om de optie uit te oefenen. Er zijn verschillende typen optie, maar de belangrijkste twee zijn de call (koopoptie) en de put (verkoopoptie). De call geeft de houder het recht om het onderliggende product van de optie tegen een vooraf vastgestelde prijs te kopen, terwijl de put aan de houder het recht geeft om het onderliggende product te verkopen voor een vastgestelde prijs. Dit alles kan gebeuren op een vastgesteld tijdstip, de expiratiedatum, waarbij men dan spreekt van een Europese optie, ofwel dit kan gebeuren binnen de tijd voor de expiratiedatum, waarbij men spreekt van een Amerikaanse optie. Opties zijn onderhavig aan stochastische processen, omdat de aandeelprijs een stochastische variabele is. Door bepaalde aannames te maken, kan de deterministische Black-Scholes vergelijking worden opgesteld, die de prijs bepaalt van een Europese optie met de uitoefenprijs, volatiliteit, rente, expiratiedatum en het dividend als parameters. Deze vergelijking heeft voor Europese opties een exacte oplossing en kan uitstekend gebruikt worden om een numerieke methode te ontwikkelen. Numerieke methoden zijn noodzakelijk om de oplossing van een Amerikaanse optie te verkrijgen of om de waarde van een optie op een mandje met aandelen te bepalen. Hierbij zijn de nauwkeurigheid en de convergentie van de numerieke oplossing van essentieel belang. Problemen, die bij het numeriek oplossen van de voornoemde vergelijking optreden, zijn onder andere een niet differentieerbare eindvoorwaarde en een rand in het "oneindige". Door lokale verfijning toe te passen middels een coördinaten transformatie, kan een zeer accurate vierde orde methode gecreëerd worden op een rooster van niet meer dan 50 punten. Om een nauwkeurigheid van minder dan een cent in de gewenste optiewaarde te verkrijgen (vergeleken met een analytische oplossing), zijn minder roosterpunten al voldoende. De waarden van exotische Europese opties kunnen eveneens met deze methode nauwkeurig bepaald worden, zodat de methode geschikt lijkt voor opties op meerdere aandelen en Amerikaanse opties. De eerder genoemde volatiliteit is een onbekende parameter die betrekking heeft op de aandelenkoers in de toekomst. Met de bekende optiewaarde (bijvoorbeeld uit de krant), is de volatiliteit de enige onbekende paremeter in de vergelijking. De combinatie van een snelle numerieke methode en een snel convergerend niet-lineair iteratieproces kan ingezet worden om de bijbehorende volatiliteit te vonden in minder dan tien iteratieslagen.

Contents

List of Figures

List of Tables

List of symbols

Greek Symbols

Γ	Gamma:Second order derivative of the option price. One of the Greeks
Δ	Delta: First order derivative of the option price, One of the Greeks
α	Coefficient in front of the second order derivative terms.
β	Coefficient in front of the first order derivative terms.
γ	Coefficient in front of the other terms in the PDE
δ	Continuous dividend yield.
ν	Stretching parameter
σ	Volatility

Latin symbols

C	Price of a call option
E	Exercise price
M	Amount of money on the bank
P	Price of a put option
S	Asset price
T	Exercise time
V	General option price
W	Wiener Process
r	Risk-free interest rate
t	Time coordinate
u	Numerical solution

Chapter 1

Introduction

Options are widely used on markets and exchanges. The famous Black-Scholes model is a convenient way to calculate the price of an option. In this thesis a highly accurate numerical method to solve this equation will be presented. Although the exact solution of the Black-Scholes equation is known, a numerical method will be proposed. A reason is to create a general numerical model for many different types of options. In particular, American options are not solvable in an analytic sense. If the numerical method works for European style option, then this is the basis to get the solution for an American option. Another issue is "implied volatility". Volatility is a quantitative expression for the randomness in the market. From newspapers or stock exchanges, the volatility of asset prices in the future is not known, so it has to be estimated. If we have a value for the option price, it is possible to calculate the volatility, which is the only unknown parameter in the Black-Scholes equation.
The main questions dealt with in this thesis are:

- Can we use fewer than 50 grid points to calculate the value of an option with a reliable accuracy by setting up a high order discretization in space and time and by employing grid stretching around interesting regions?

- Will the highly accurate numerical scheme also work for exotic options with discontinuous final conditions?

- Can we calculate the implied volatility by some iterative methods in only a few iterations?

The contents of this thesis will now be described. After this introduction, in chapter 2, the definitions and properties of options and some economical aspects are discussed. Section 2.1 deals with the description of forward contracts and options. In Section 2.2, some important definitions from economics are discussed.
Chapter 3 discusses the derivation of the mathematics regarding options and their prices.

Section 3.1 describes the stochastic model of asset prices based on which the Black Scholes equation for option prices will be derived in section 3.2. Section 3.3 shows some options used and the mathematical properties of these options. The derivatives of the option price are very important, which will be explained in section 3.4.
Chapter 4 shows our numerical setup for the in chapter 3 derived equations. Section 4.1 deals with the space discretization of a general parabolic differential equation. In section 4.2., transformation techniques are discussed. The chapter will conclude with the time integration methods and initialization techniques in section 4.3.
Chapter 5 shows the results of three reference test problems of diffusion type, on which the numerical schemes derived in chapter 4 are applied.
In chapter 6, some specific numerical issues about the Black-Scholes equation will be discussed. It contains some subjects, which we have to tackle in our problems.
In chapter 7 the numerical results of the option pricing experiments are shown systematically. The thesis will, be concluded with conclusions in chapter 8. In the appendix (part 2), formulas for the derivatives of all options and the Matlab software code for the experiments in chapter 7 are placed.

Chapter 2

Options and Finance

This chapter is an introduction to the computational finance subjects in this thesis. Before a mathematical description, it is necessary to clarify some economical definitions. First, the main topic of this thesis, option contracts and the pricing of options will be discussed.

2.1 Financial contracts and options

Many different financial contracts exist. A *forward contract*, for example, is an agreement to buy or sell an asset for a certain price at a certain time in the future. It is related to a *spot contract* which is an agreement to buy or sell an asset today (e.g. buying bread at the bakery). The participants in forward contracts are the *holder* and the *writer*. The holder, who buys the contract takes a *long position* on the asset. The writer sells the option and takes a *short position*. A forward contract is binding towards both parties: the holder is obliged to buy the asset and the writer is obliged to sell the asset. This is not the case in option contracts.

Options give the holder the **right** to exercise the option, so he is not obliged to buy the asset. The writer is, however obliged to sell the asset. There are two basic types of options: the *call* and the *put*. A call option is an option which gives the holder the right to *buy* an asset for a certain price. A put option gives the holder the right to *sell* an asset for a certain price. The price mentioned in both option contracts is called the exercise price, E. The most commonly traded types of calls and puts are European and American options. Therefore these options are also called "vanilla" options. In the case of European options, the holder may only exercise the option at the time of maturity or exercise time, T. American options may be exercised in the period before maturity.

Options are used for several purposes. The two most important are speculating and hedging. Speculation may be easy to understand: if the holder buys a call, he expects that the stock price will increase. The exercise price will be E. If the stock price S is greater than E, the call will be exercised and the net profit of the option will be $S-E-C$, where

C is the cost of the option. C is an important parameter in the Black-Scholes analysis in chapter 3. Speculation with options involves a greater risk than speculation with assets: the profit and losses are typically larger when using options.
The second purpose to use options is "hedging". The following example taken from [10] may clarify hedging. Suppose an investor has 500 shares of a company. The current share price is € 102. If the investor expects the stock price to decrease, he may buy 500 put options with exercise price € 100 to ensure this portfolio against a possible falling asset price. The option price is, for example, € 4.
So, his costs will be 500× € 4 =€ 2.000. Now, suppose the stock price falls below € 100, then the puts give a guaranteed value of the portfolio (see section 2.2) of € 50.000 - € 2.000=€ 48.000. Otherwise, if the stock price stays above € 100, the options will not be exercised and the value of the assets will always be above € 48.000. In this way, options are used for reducing the risk in the market. This is a typical example of hedging, i.e, using options to reduce the risk of a portfolio.

2.2 Some other economical definitions

The definition of an option contract has already been described, but some definitions still have to be clarified.

Definition 1 ***Portfolio***. *A portfolio is the collection of all shares, options and other derivatives owned by a trader.*

Definition 2 ***Arbitrage***. *Arbitrage indicates that it is not possible in a financial market to make risk-free profits larger than just placing money in the bank.*

There are several types of portfolios. One of the most important is the arbitrage portfolio which has a probability of 1 to increase in time. Shares and options are combined in such a way that risk is eliminated. This is an instantaneously risk-free money making price process. It is assumed that markets are free of arbitrage, which is also a property of the Black-Scholes analysis derived in chapter 3.
The term "risk-free" will be used in relation to the profit from the interest rate when placing money in the bank.

Definition 3 ***Risk-free interest rate*** *The risk-free interest rate, $r(t)$, is the growth of money, M in time.*

$$M(t) = E \exp(-\int_0^t r(t)dt) \tag{2.1}$$

Due to "supply and demand" there will be a range of interest rates which causes the financial market to be arbitrage free (for details, see [1] chapter 2). In the scope of this thesis $r(t)$ will be a constant value.
Of course, also dividend payment and randomness in the market play an important role.

Figure 2.1: Index of KPN stock over the last 5 years with high and low volatility region, related to the AEX index.

Definition 4 ***Dividend***. *Dividend,δ, will be received by the owner of a share of some profit making company. Typically, the stock price will decrease when dividend is paid.*

Definition 5 ***Volatility***, *σ is related to the standard deviation of the stock price of a share. It is an indication for the random behaviour of the market.*

Option prices are based on stochastic models for asset prices. Two economists, Scholes and Merton, won the Nobel-prize (1997) for their model to compute the option price. (Black died 1995)
In chapter 3, we will see that the value of an option, or option price, will be a function of the stock price, S, the time to maturity, T, the risk-free interest rate r, the dividend payment δ and the volatility, σ. One of the important factors in the Black-Scholes equation will be the volatility. Because the value of an option depends on asset prices in the future, the volatility (uncertainty in the market) should be modeled. Typically, it is not always possible to estimate the volatility based on the history of the asset prices. The uncertainty of the volatility in the future, gives rise to many different models for the asset prices (and also for the option prices), see, for example, [10]. In the Black-Scholes analysis in chapter 3, a constant volatility is assumed.

Chapter 3

Black-Scholes analysis

In this chapter the Black-Scholes equation will be derived to obtain the value of an option. Using the definitions about options from the chapter 2, boundary and final conditions for the options can be stated. Especially these conditions distinguish the different types of options.

3.1 Stochastic model

First of all, the price process for assets is described. It is modeled by a stochastic differential equation based on a geometric Brownian motion (see, for example, chapter 2 of [19]). The "asset price" is the price of the underlying of an option. The change or price difference in the asset prices is assumed to be a Markov-process.

Definition 6 *The **return** is the change in the price divided by its original value:* $\frac{dS}{S}$

In the so-called Samuelson model [19], there are two contributions to the return: a deterministic and a stochastic contribution. If ν is the average rate of growth of the asset price, also known as the "drift", the deterministic contribution in time dt is found to be νdt. The other contribution relates to the random change in the asset prices. With σ the volatility related to the standard deviation of the returns and dX a sample from a normal distribution, the contribution is assumed to be σdX. The resulting equation reads

$$\frac{dS}{S} = \nu dt + \sigma dX. \tag{3.1}$$

This is a *stochastic differential equation*. The normal distribution used in (3.1) is a Wiener process with the following properties: $E(dX) = 0$ and $E(dX)^2 = dt$. To see that σ is proportional to $Var(dS)$, the expectation and the variance are calculated as

$$E(dS) = E(\nu S dt + \sigma S dX) = E(\nu S dt) + E(\sigma S dX) = \nu S dt \quad (E(dX) = 0)$$
$$Var(dS) = E(dS^2) - (E(dS))^2 = E((\nu S dt + \sigma S dX)^2) - (\nu S dt)^2 = \sigma^2 S^2 dX^2,$$

since $E(S^2 dX dt) = 0$. The standard deviation is the square-root of the variance, so σ is proportional to $\frac{\sqrt{Var(dS)}}{S}$.

3.2 Partial differential equation

Consider a general option value $V(S,t)$. The Taylor-expansion reads:

$$dV = \frac{dV}{dS}dS + \frac{dV}{dt}dt + \frac{1}{2}\frac{d^2V}{dS^2}dS^2 + \cdots \tag{3.2}$$

From equation (3.1) it follows that

$$\begin{aligned} dS^2 &= (\nu S dt + \sigma S dX)^2 \\ &= \nu^2 S^2 dt^2 + 2\sigma\nu S^2 dX dt + \sigma^2 S^2 dX^2. \end{aligned} \tag{3.3}$$

Then, by applying Ito's Lemma (see, for example, [3]) and the assumption that $dX^2 \to dt$ as $dt \to 0$, with probability 1, equation (3.3) reads to leading order

$$dS^2 \to \sigma^2 S^2 dt. \tag{3.4}$$

Inserting (3.4) into (3.2), it follows that

$$dV = \sigma S\frac{\partial V}{\partial S}dX + (\nu S\frac{\partial V}{\partial S} + \frac{1}{2}\sigma^2 S^2\frac{\partial^2 V}{\partial S^2} + \frac{\partial V}{\partial t})dt. \tag{3.5}$$

This is the random walk process for V. Now, by setting up a portfolio consisting of one option with value V and a number $-\Delta$ of the underlying asset. The value of this portfolio will be

$$\Pi = V - \Delta S \tag{3.6}$$

and the change in the portfolio reads

$$d\Pi = dV - \Delta dS. \tag{3.7}$$

Combining (3.1), (3.5), (3.6) and (3.7), it follows that:

$$d\Pi = \sigma S\left(\frac{\partial V}{\partial S} - \Delta\right)dX + \left(\nu S\frac{\partial V}{\partial S} + \frac{1}{2}\sigma^2 S^2\frac{\partial^2 V}{\partial S^2} + \frac{\partial V}{\partial t} - \nu\Delta S\right)dt. \tag{3.8}$$

To eliminate the main contribution of randomness, one chooses

$$\Delta = \frac{\partial V}{\partial S}. \tag{3.9}$$

In section 3.4 this value Δ will be discussed as an important hedge parameter. With Δ chosen as in (3.9), the portfolio (3.6) is deterministic, i.e. it is instantaneously risk free. The change in an instantaneously risk free portfolio should equal the exponential growth of placing of placing money in the bank. So,

$$d\Pi = r\Pi dt = (\frac{1}{2}\sigma^2 S^2 \frac{\partial^2 V}{\partial S^2} + \frac{\partial V}{\partial t})dt. \tag{3.10}$$

Finally after inserting (3.6) into (3.10) and dividing by dt, the famous **Black-Scholes** equation for valuing an option with value V is obtained

$$\frac{\partial V}{\partial t} + \frac{1}{2}\sigma^2 S^2 \frac{\partial^2 V}{\partial S^2} + rS\frac{\partial V}{\partial S} - rV = 0 \tag{3.11}$$

A short way of writing (3.11) is

$$\frac{\partial V}{\partial t} + \mathcal{L}_{BS} V = 0. \tag{3.12}$$

Properties of this equation and assumptions in the analysis are:

1. The equation is a linear parabolic partial differential equation with non-constant coefficients and (to be discussed in section 3.3) non-homogeneous boundary conditions and, possibly, non-differentiable or even discontinuous final conditions.

2. The asset price follows the log-normal distribution which arises from (3.1)

3. The risk-free interest rate r and the volatility σ are both known functions of time over the life of the option.

4. Transaction costs associated with hedging are not included

5. There is no dividend payment (the basic model assumes no dividend payment, but a simple modification can be made to include some form of dividend payment)

6. It is assumed that there are no arbitrage possibilities

7. Trading of the underlying can take place continuously.

8. Short selling is possible, which means that assets may be sold without possessing them.

One of the important drawbacks of this model is that the volatility is assumed to be a constant function. In reality this is not the case, but for many options the Black-Scholes model can still be successfully used. Currently there is a lot of research on more accurate modeling of asset price processes by inclusion of jumps or stochastic volatility in the asset

price processes, see for example, [10]. These models can handle the aspect of non-constant volatility more accurately. The improved asset models have an important impact on the equations for option prices. Improved modeling is, however, beyond the scope of this thesis.
When a constant dividend payment is assumed, there will be only a slight change to the general Black-Scholes equation. Taking the same function Π as equation (3.6) and consider a constant dividend payment δS, we change the definition of $d\Pi$, as:

$$d\Pi = dV - \Delta dS - \delta S \Delta dt. \tag{3.13}$$

The Black-Scholes PDE reads in this case

$$\frac{\partial V}{\partial t} + \frac{1}{2}\sigma^2 S^2 \frac{\partial^2 V}{\partial S^2} + (r - \delta) S \frac{\partial V}{\partial S} - rV = 0. \tag{3.14}$$

This dividend payment is some ratio of the asset price and it can be interpreted as some kind of interest rate. This dividend payment is mainly useful for options on an index. In that case, one can assume a continuous dividend payment. Otherwise, in the case of options on regular stocks it make sense to include a discrete dividend payment which takes place only once or twice a year, for example.

3.3 Different types of options

Parabolic equations (3.11) or (3.14) are second order partial differential equations in S-space and first order in time. One final (or initial) and two boundary conditions are necessary. As known from standard literature on partial differential equations (see [2] or [17]), a diffusion equation of this type is ill-posed if it comes with an initial condition. However, option problems have final conditions. The boundary and the final conditions make the difference between American and European style as well as between put and call and other types of options. The Black-Scholes equation (3.11) is a convection-diffusion-reaction equation of a special form. American options are out of the scope of this thesis. For convenience, the value of a call option will be denoted by C and of a put option by P.

3.3.1 European Call

As described in chapter 2, a call option gives the holder the right to exercise his option at maturity time, T. To buy the underlying asset at maturity time T makes sense if the asset price is higher than the exercise price ($S > E$). One can buy the asset for E and sell it immediately on the market for S. If this is not the case, then the option is worthless. The value of the option is thus known at maturity time, namely it is either zero or $S - E$, which is the net amount of profit. So, the final condition for a call is known (and

the problem is a well-posed problem). The boundary conditions follow from economical arguments. If $S = 0$,the value of the call option equals zero. For S tends to infinity, the holder will exercise and the value of his option will be simply the asset price corrected by the dividend minus the exercise price corrected by the case if the holder had invested his money on the bank, so $C(S,t) = Se^{-\delta(T-t)} - Ee^{-r(T-t)}$. This is the right-hand boundary. Summarizing the problem reads

$$\begin{aligned} &\frac{\partial C}{\partial t} + \mathcal{L}_{BS}C = 0 \\ &\qquad C(0,t) = 0 \\ &\qquad C(S,t) = Se^{-\delta(T-t)} - Ee^{-r(T-t)} \quad \text{as } S \to \infty \\ &\qquad C(S,T) = \max(S-E,0) = \begin{cases} S-E & S > E \\ 0 & S \leq E \end{cases}. \end{aligned} \tag{3.15}$$

From [19], the analytic solution of the call option is known and reads:

$$C(S,t) = Se^{-\delta(T-t)}N(d_1) - Ee^{-r(T-t)}N(d_2), \tag{3.16}$$

with the notations:

$$d_1 = \frac{\ln S - \ln E + \left(r - \delta + \frac{1}{2}\sigma^2\right)(T-t)}{\sigma\sqrt{T-t}} \tag{3.17}$$

$$d_2 = d_1 - \sigma\sqrt{T-t} \tag{3.18}$$

$$N(y) = \frac{1}{\sqrt{2\pi}} \int_{-\infty}^{y} e^{-\frac{1}{2}x^2} dx. \tag{3.19}$$

The parameter $N(d_2)$ denotes the probability that the asset price will be above the exercise price (see [1]). In figure 3.1, the solution of a call option has been plotted. Next to the final condition at $t = T$, C at $t = 0$ is presented for an option $E =$€ 15, $\sigma = 0.3$, $r = 0.05$, $\delta = 0.03$ and $T = 2.0$.

3.3.2 European Put

A European put option gives the holder the right to sell the underlying asset for the strike price E at maturity time T. If the asset price is more than the exercise price, the option is worthless, so $P(S,T) = 0 \quad \forall S > E$. If the asset price is below the exercise price, the

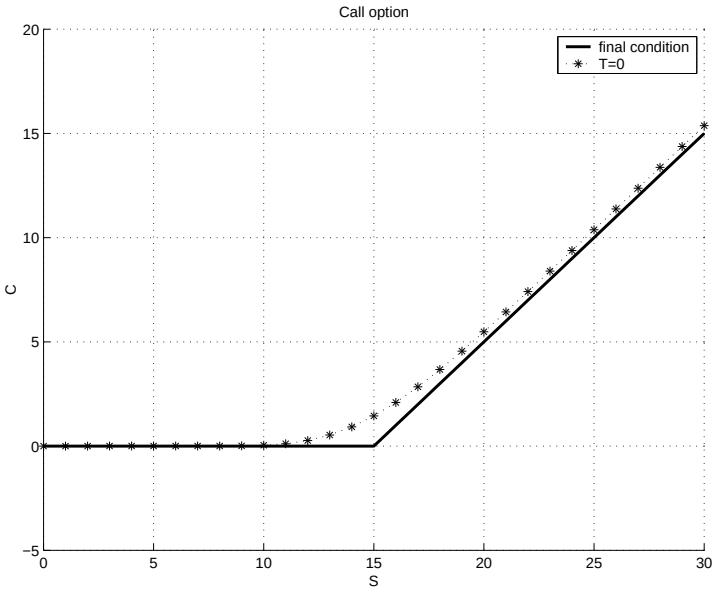

Figure 3.1: Final value and solution for a European call.
Parameters are $E = 15, \sigma = 0.3, r = 0.05, \delta = 0.03, T = 2.0$

net profit is $E - S$. The boundary conditions again follow from economical arguments.

$$\begin{aligned} &\frac{\partial P}{\partial t} + \mathcal{L}_{BS} P = 0 \\ &\qquad P(0,t) = Ee^{-r(T-t)} \\ &\qquad P(S,t) = 0 \quad \text{as } S \to \infty \\ &P(S,T) = \max(E-S,0) = \begin{cases} E-S & S < E \\ 0 & S > E \end{cases}. \end{aligned} \tag{3.20}$$

From [19] and with d_1, d_2, N from (3.17), (3.18) and (3.19) the analytic solution of the put option reads

$$P(S,t) = Ee^{-r(T-t)} N(-d_2) - Se^{-\delta(T-t)} N(-d_1). \tag{3.21}$$

In figure 3.2, the graph of a put option has been plotted for the same parameters as in figure 3.1. Put and call option prices are related via the *Put-Call parity* relation, which states that:

$$C(S,t) + Ee^{-r(T-t)} = P(S,t) + Se^{-\delta(T-t)}. \tag{3.22}$$

This relation is based on the arbitrage principle (see, for example, [19]): At $t = T$ the value of both, the left- and right-hand side are certain. $\max(S-E,0)+E = \max(E-S,0)+S$.

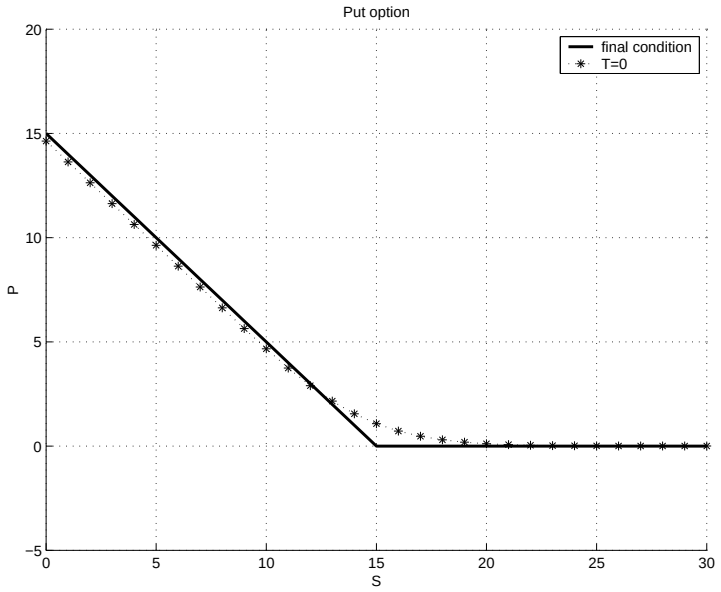

Figure 3.2: Final value and solution for a European put. Parameters as in figure 3.1

If $S > E$, the left-hand side becomes S, as well as the right-hand side; if $S < E$, the right-hand side equals E as well as the left-hand side. With this an arbitrage risk-free portfolio can be composed.

3.3.3 Digital Call options

Another option is the *digital call option*. This option belongs to the so-called class of exotic options. These options are not traded at exchanges, but such contracts are traded between a bank and a customer. Nowadays, a large variety of exotic options exists. They are typically characterized by different boundary or final conditions than from the standard or vanilla European options. We examine the digital option because of its discontinuous payoff. The principle is simple. If the stock price is higher than the exercise price E, the holder receives a fixed amount Q ($Q = 1$ for pure digitals). So, if a holder pays € 0.50 for a digital call and the asset price is above the exercise price, the holder makes a net profit of € 0.50. These types of options are not useful in American style, because, the options are immediately exercised, if the asset price increases above the exercise price. The final condition for a digital call option is the Heaviside function, $\mathcal{H}(S)$: $C = 1$ if $S > E$ and $C = 0$ if $S < E$. The left boundary is the same as the usual call, $C(0, t) = 0$ and the right boundary is only the payoff amount corrected by the interest rate (see [10]).

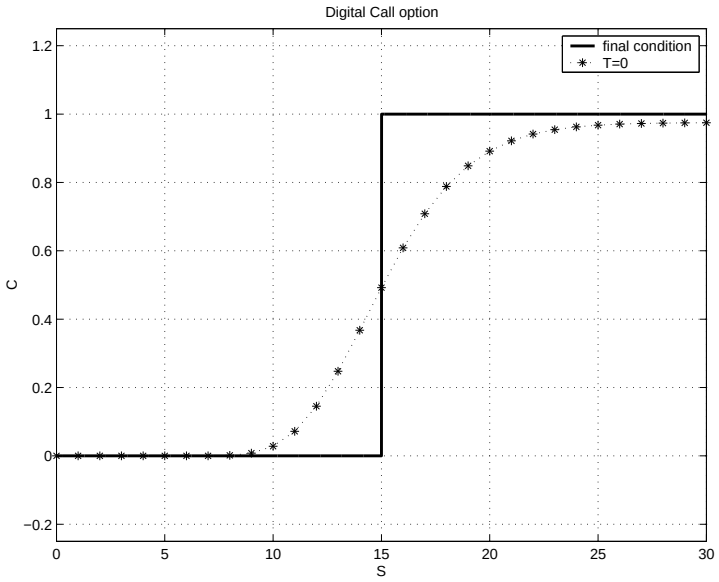

Figure 3.3: Final value and solution for a European digital call. Parameters are $E = 15, \sigma = 0.3, r = 0.05, \delta = 0, T = 2$.

Summarizing:

$$\begin{aligned} \frac{\partial C}{\partial t} + \mathcal{L}_{BS} C &= 0 \\ C(0,t) &= 0 \\ C(S,t) &= Qe^{-r(T-t)} \quad \text{as } S \to \infty \\ C(S,T) &= Q\mathcal{H}(S-E) = \begin{cases} Q & S > E \\ 0 & S < E \end{cases}. \end{aligned} \tag{3.23}$$

From [10] and with with d_1, N from (3.17) and (3.19), the analytic solution of the digital call option reads:

$$C(S,t) = Qe^{-r(T-t)} N(d_2) \tag{3.24}$$

In figure 3.3 the final condition and the solution at $t = 0$ of a digital call option have been plotted for $E = 15, \sigma = 0.3, r = 0.05, \delta = 0, T = 2$. A second type of digital call option, is the asset or nothing call. This option is also available in American style. If the asset price is below the exercise price at maturity time, the option is worthless $C(S < E, T) = 0$. When the asset price is above the exercise price the payoff equals $C(S > E, T) = S$. The right boundary condition equals S corrected by the dividend ratio. The left boundary

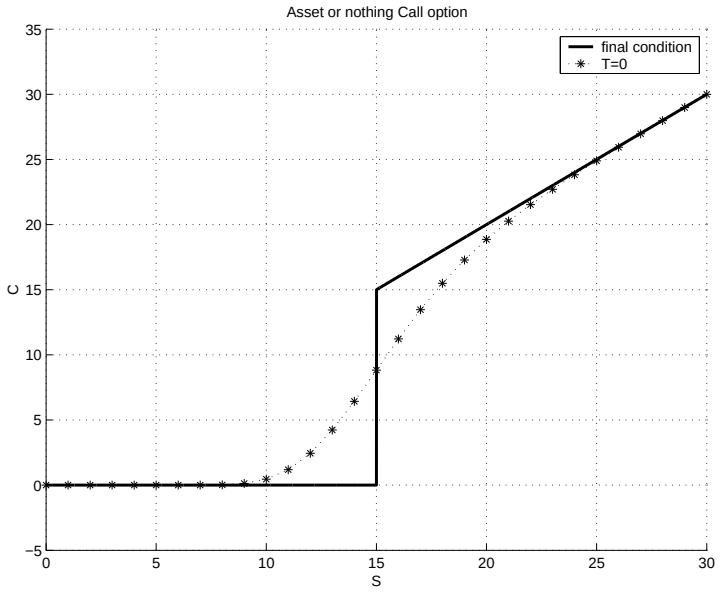

Figure 3.4: Final value and solution for a European asset or nothing call. Parameters as in figure 3.3

equals zero (again from economical arguments). Summarizing:

$$\begin{aligned} &\frac{\partial C}{\partial t} + \mathcal{L}_{BS} C = 0 \\ &\qquad C(0,t) = 0 \\ &\qquad C(S,t) = S e^{-\delta(T-t)} \quad \text{as } S \to \infty \\ &\qquad C(S,T) = S\mathcal{H}(S-E) = \begin{cases} S & S > E \\ 0 & S < E \end{cases} \end{aligned} \tag{3.25}$$

From [10], the solution of the asset or nothing call option reads:

$$C(S,t) = S e^{-\delta(T-t)} N(d_1) \tag{3.26}$$

In figure 3.4 the final condition and the solution at $t = 0$ of an asset or nothing call option have been plotted.

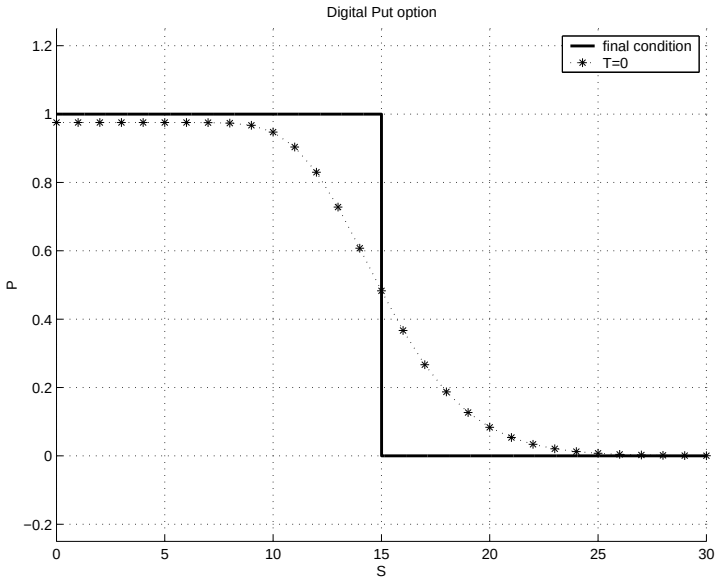

Figure 3.5: Final value and solution for a European digital put. Parameters as in figure 3.3

3.3.4 Digital Put options

In analogy the digital put exists. The equation for the digital put reads:

$$\begin{aligned} &\frac{\partial P}{\partial t} + \mathcal{L}_{BS} P = 0 \\ &\qquad P(0,t) = Q e^{-r(T-t)} \\ &\qquad P(S,t) = 0 \quad \text{as } S \to \infty \\ &P(S,T) = Q\left(1 - \mathcal{H}(S-E)\right) = \begin{cases} 0 & S > E \\ Q & S < E \end{cases} \end{aligned} \tag{3.27}$$

From [10], the analytic solution of the digital put option reads:

$$P(S,t) = Q e^{-r(T-t)} N(-d_2) \tag{3.28}$$

In figure 3.5 the final condition and the solution at $t = 0$ of a digital put option have been plotted. Also the asset or nothing variant of this option exists. This equation reads

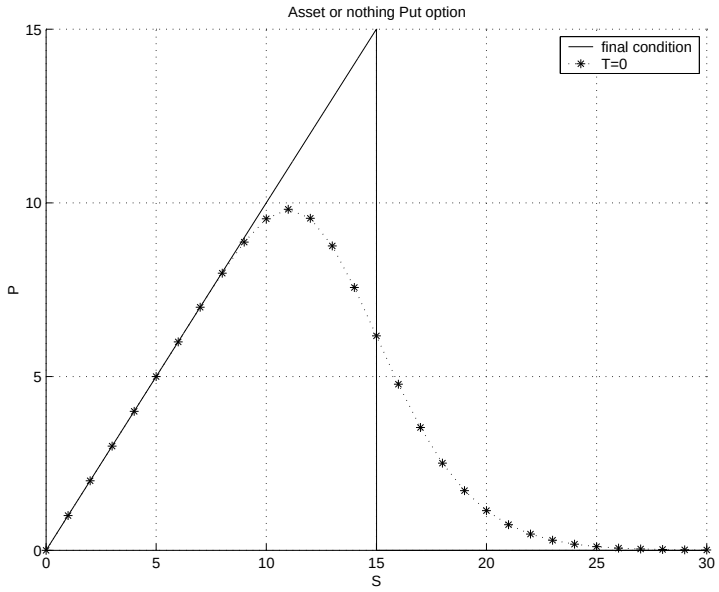

Figure 3.6: Final value and solution for a European asset or nothing put. Parameters as in figure 3.3

$$\begin{aligned} &\frac{\partial P}{\partial t} + \mathcal{L}_{BS} P = 0 \\ &\qquad P(0,t) = S e^{-\delta(T-t)} \\ &\qquad P(S,t) = 0 \quad \text{as } S \to \infty \\ &P(S,T) = S\left(1 - \mathcal{H}(S-E)\right) = \begin{cases} 0 & S > E \\ S & S < E \end{cases} \end{aligned} \tag{3.29}$$

From [10], the solution of the asset or nothing put option will be:

$$P(S,t) = S e^{-\delta(T-t)} N(-d_1) \tag{3.30}$$

In figure 3.5 the final condition and the solution of a digital put option have been plotted.

3.3.5 Linear combinations

In this thesis, options on only one underlying asset are considered. Trading in options is typically not done with a single option, but with a variety of options. In practice, trading a combination of options on the same underlying is a very common strategy. Mostly traded are the so-called *spreads*. A spread is a combination of two (or more) options with different exercise prices E and both in a long position as well as in a short position, i.e.

a trader acts as a holder and as a writer in this situation. All options have the same maturity time. The *Bull spread*, for example, is a long position call with an exercise price E_1 and a short position on an option with exercise price E_2, with $E_2 > E_1$. The profit for the holder and at the same time the losses for the writer are reduced with a bull spread compared to a single option (see figure 3.7). Consider as an example a long position call bought for € 3 with exercise price $E_1 =$ € 15 and a short position call sold for € 1 with exercise price $E_2 =$ € 20. The *profit* at $t = T$, defined as the payoff minus the cost of the bull spread reads

$$\text{Profit} = \begin{cases} -2 & S < E_1 \\ S - 17 & E_1 < S < E_2 \\ 3 & S > E_2 \end{cases}$$

Figure 3.7 shows the solution and the payoff for a bull spread with parameters $E_1 = 15, E_2 = 20, \sigma = 0.3, r = 0.05, \delta = 0.03, T = 0.5$. The *Bear spread* is the reverse of a bull spread; it is a combination of a long position with a higher exercise price E_2 and a short position with a lower exercise price E_1, see figure 3.8. Consider as an example a long position call bought for € 1 with exercise price $E_1 =$ € 20 and a short position call sold of € 3 with exercise price $E_2 =$ € 15. The profit is then:

$$\text{Profit} = \begin{cases} 2 & S < E_1 \\ 15 - S & E_1 < S < E_2 \\ -3 & S > E_2 \end{cases}$$

In this case the losses of the holder are reduced as well as the profit of the writer as compared to a single option. In figure 3.8 the payoff and the solution at $t = 0$ for a bear spread are presented.

The *Butterfly Spread* is a combination of four options. Two long position calls with exercise price E_1 and E_3 and two short position calls with exercise prices $E_2 = \frac{1}{2}(E_1 + E_3)$. The payoff (not the profit) reads here

$$\text{Payoff} = \begin{cases} 0 & S < E_1 \\ S - E_1 & E_1 < S < E_2 \\ E_3 - S & E_2 < S < E_3 \\ 0 & S > E_3 \end{cases}$$

An example is given in figure 3.9.

These spreads are all in some way less risky than the usual European options.
A digital spread is often called a *Supershare*. An example is a combination of a long position cash-or-nothing call with amount Q/d and exercise price E and a short position

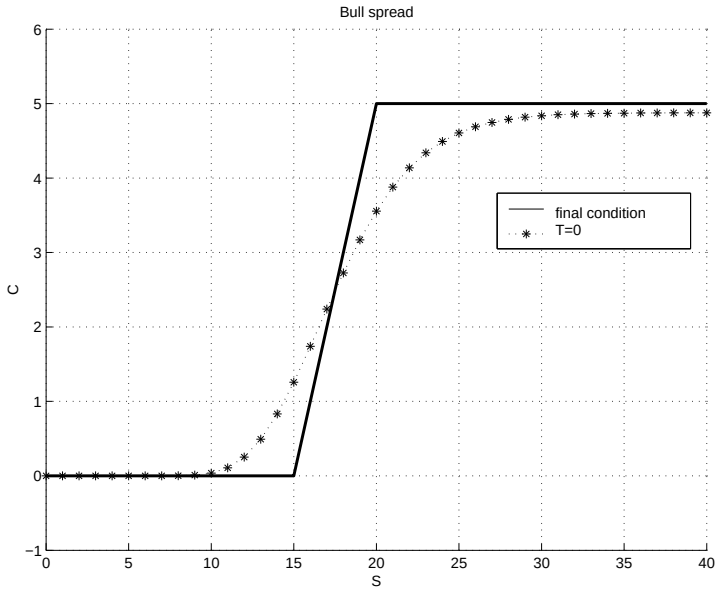

Figure 3.7: Solution and final value of a Bull Spread.
Parameters are $E_1 = 15, E_2 = 20, \sigma = 0.3, r = 0.05, \delta = 0.03, T = 0.5$

cash-or-nothing call with amount Q/d and exercise price $E + d$. The payoff is then:

$$\text{Payoff} = \begin{cases} 0 & S < E \\ Q/d & E < S < E + d \\ 0 & S > E + d \end{cases}$$

In figure 3.10 the payoff function of this spread has been plotted. Note that the values of all spreads are described by the Black-Scholes equation, because the spread strategies can be seen as linear combinations of single options. Furthermore, the equation is linear. For example, a bull spread can be computed as a combination of a long position call and, separately, a short position call. The value of the spread is just a linear combination of the results of these computations.

3.3.6 Barrier Options

Barrier options are also different from European vanilla options. They belong to the exotic options too. In this thesis a "down and out barrier" option will be discussed. A down and out option is worthless if the asset price falls below a barrier amount B (which will be less than E in the example to be discussed). So, the option is worthless if $S < B$ and therefore the left side boundary condition will change to $V(B, t) = 0$ instead of $V(0, t) = 0$. (V has been used instead of C). The only modification is that the differential equation has to be

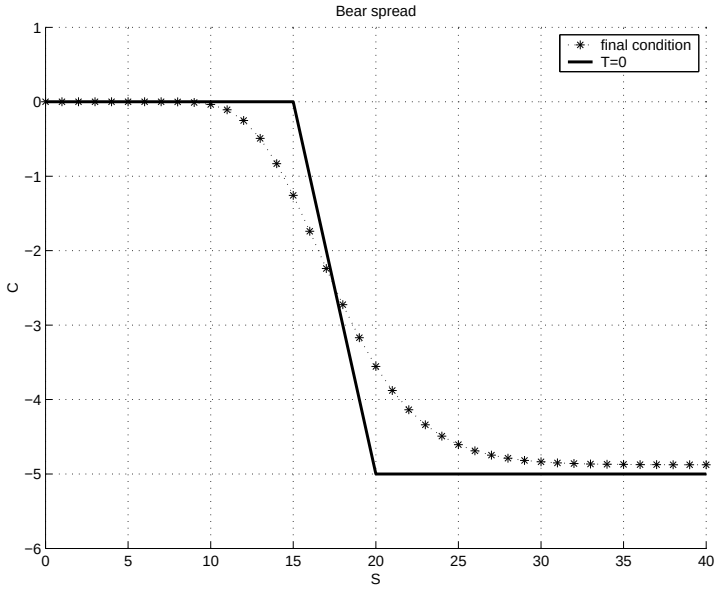

Figure 3.8: Solution and final value of a Bear Spread.
Parameters are $E_1 = 15, E_2 = 20, \sigma = 0.3, r = 0.05, \delta = 0.03, T = 0.5$

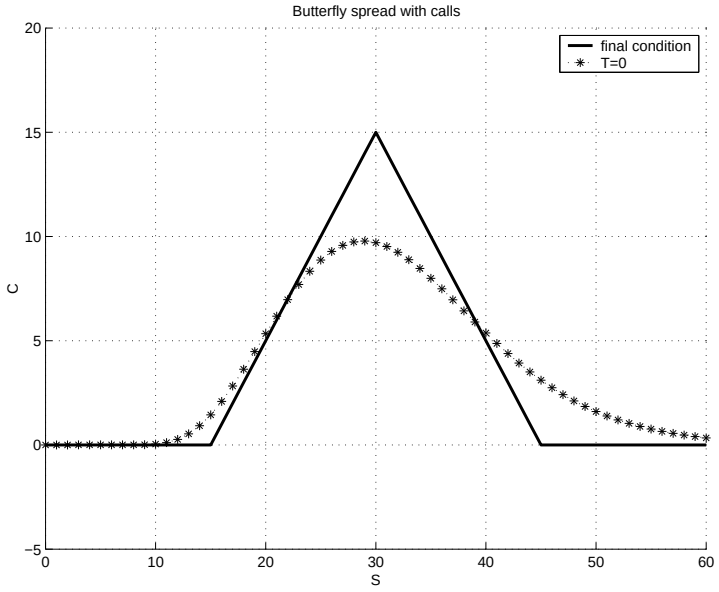

Figure 3.9: Solution and final value of a Butterfly Spread.
Parameters $E_1 = 15, E_2 = 30, E_3 = 45, \sigma = 0.3, r = 0.05, \delta = 0.03, T = 0.5$.

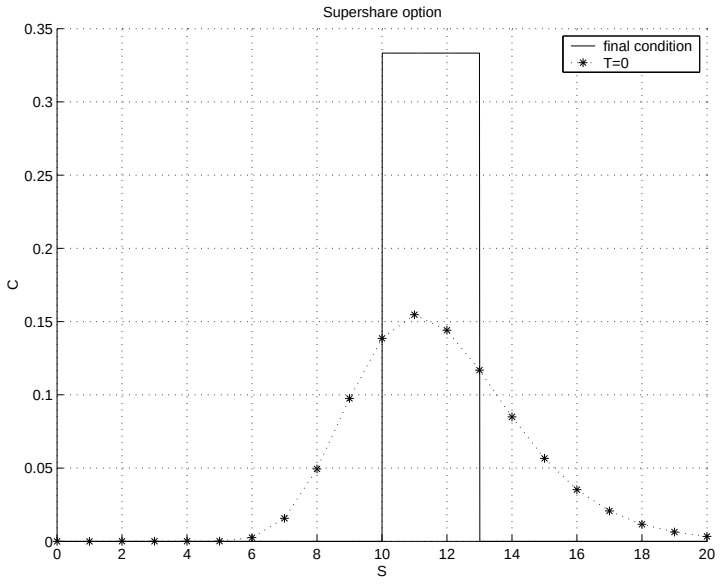

Figure 3.10: Solution and final value of a Super share.
Parameters $E = 15, d = 3, \sigma = 0.3, r = 0.05, \delta = 0, T = 0.5$.

solved in the region $S \in [B, S_{max}]$. The exact solution reads (see [19]):

$$V(S,t) = C(S,t) - \left(\frac{S}{B}\right)^{-(k-1)} C\left(\frac{B^2}{S}, t\right), \tag{3.31}$$

where $C(S,t)$ denotes the solution of the standard European call and $k = \dfrac{2r}{\sigma^2}$

3.4 The Greeks

In the introduction of this thesis, the term hedging has been explained. In the derivation of the Black-Scholes equation, the elimination of the randomness in the option pricing process is employed to derive the deterministic Black-Scholes equation. The quantity that eliminates the main contribution to randomness in this model, $\Delta = \frac{\partial V}{\partial S}$ is one of the important parameters in option pricing. It is the rate of change of the option price with respect to the price of the underlying asset. It indicates the number of shares that should be kept with each option issued in order to cope with a loss in the case of exercise.

Another important parameter is the derivative of Δ, called Γ. It is defined by the rate of change of the portfolio's Δ with respect of the price of the underlying asset. Γ is an indication of the sensitivity of Δ. If Γ is low, it is only necessary to change sometimes the portfolio. If it is high, the portfolio under consideration results only for a very short

period of time in a risk-less scenario. These parameters are known as the Greeks. The Greeks are given by:

$$\Delta = \frac{\partial V}{\partial S}, \tag{3.32}$$

$$\Gamma = \frac{\partial^2 V}{\partial S^2}, \tag{3.33}$$

$$\Theta = \frac{\partial V}{\partial t}, \tag{3.34}$$

$$\mathcal{V} = \frac{\partial V}{\partial \sigma}, \tag{3.35}$$

$$\rho = \frac{\partial V}{\partial r}, \tag{3.36}$$

Θ is defined as the rate of change of the option price with respect to time when all other parameters are kept fixed (this the famous famous economic property *Ceteris Paribus*). $\mathcal{V}$ is known as "Vega" defined as the rate of change of the option price with respect of volatility of the underlying asset and ρ is defined by the rate of change of the option price with respect of the interest rate in the market. In this thesis, the values of Δ and Γ are investigated. The exact solution of the Greeks for European options, can be determined by writing down the differentiation of the analytic solutions of V. For a European call the analytic expressions of the Greeks are:

$$\begin{aligned}
\Delta &= e^{-\delta(T-t)} N(d_1) \\
\Gamma &= e^{-\delta(T-t)} \frac{N'(d_1)}{\sigma S\sqrt{T-t}} \\
\Theta &= -\frac{SN'(d_1)\sigma e^{-\delta(T-t)}}{2(T-t)} + \delta S N(d_1) e^{-\delta(T-t)} - rSe^{-r(T-t)} N(d_2) \\
\mathcal{V} &= e^{-\delta(T-t)} S\sqrt{T-t} N'(d_1) \\
\rho &= S(T-t)e^{-r(T-t)} N(d_2)
\end{aligned} \tag{3.37}$$

With $N'(x)$ the derivative of (3.19) which is the normal distribution. In figure 3.11-3.13 several Greeks are plotted for the parameter set used in figure 3.1 . Numerically, it is challenging to find accurate approximations of the Greeks. Since they are obtained by a numerical differentiation of the primary unknown V, the accuracy of these derivatives is not obvious beforehand. Usually, numerical differentiation reduces the order of accuracy. With second order accurate solutions Γ may be of only $\mathbf{O}(1)$, which is not satisfactory. Often, in numerical experiments, one sees that the accuracy of the Greeks is better than expected, probably due to the smoothness of the solutions. With highly accurate discretizations, however, we expect reasonable accuracy of the hedging parameters.

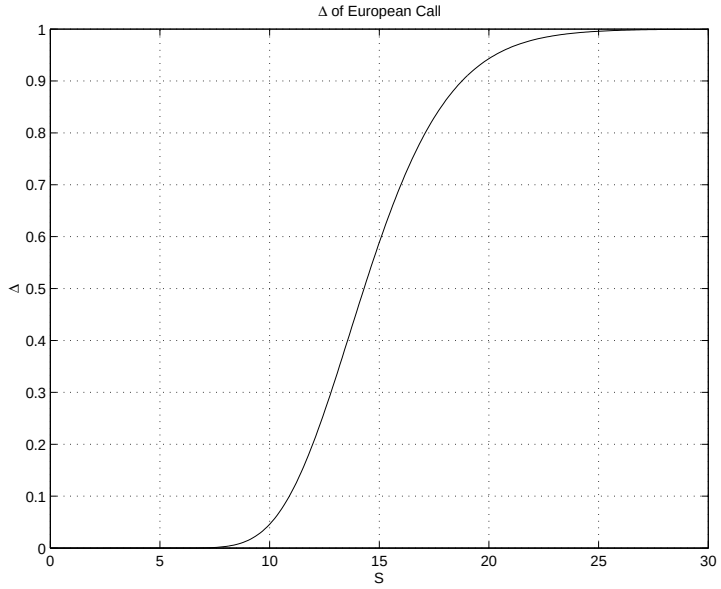

Figure 3.11: Δ of a European call. Parameters as in figure 3.1

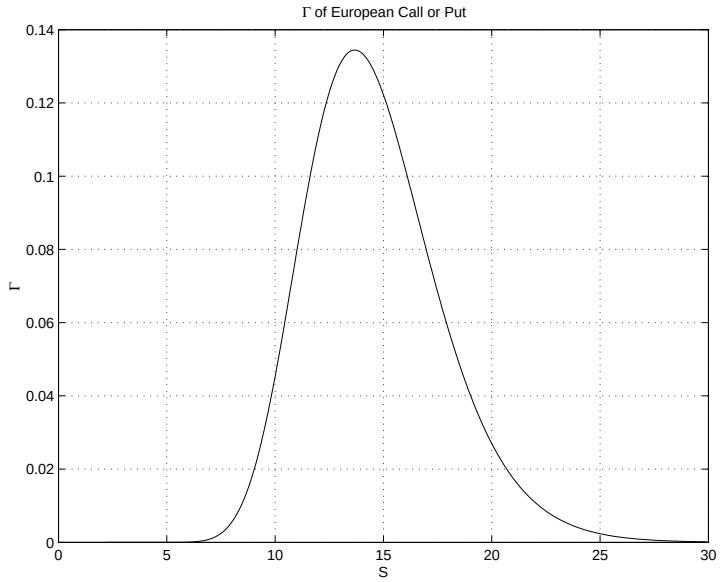

Figure 3.12: Γ of a European call. Parameters as in figure 3.1

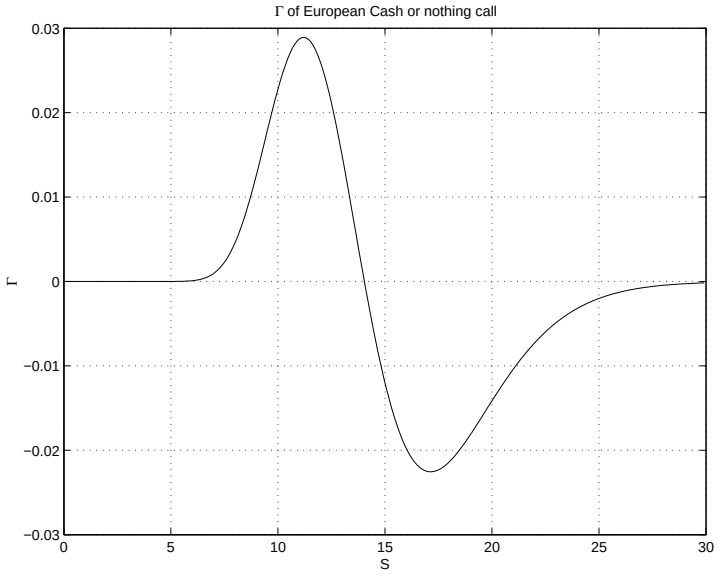

Figure 3.13: Γ of a cash-or-nothing call. Parameters as in figure 3.3

Chapter 4

Discretization of the PDE

In this chapter, a numerical method will be developed to get a fast solution of the Black-Scholes equation. A second order accurate solution, which means that the error decreases quadratically, is used in many practical situations. However, when applicable, a fourth order accurate solution will be more preferable as the numerical solution is often obtained faster as fewer grid points are necessary for the same accuracy. Also grid stretching is powerful technique to get many grid points in the region of interest. The goal is to discretize the equation in space and in time after which the resulting linear algebraic system has to be solved for each time step. The matrix equation is solved with a direct solution method, because a sparse matrix results from a one dimensional space discretization (see [16]). Iterative methods are mandatory for American options (and for certain exotic options that lead to higher dimensional PDE problems). They are out of the scope of this thesis, but in chapter 5 and 7, some properties of the matrix will be given, to determine which discretization is beneficial for iterative methods.

4.1 Space discretization

Consider a general form of a parabolic partial differential equation with non-constant coefficients, Dirichlet boundary conditions and an initial condition:

$$\frac{\partial u}{\partial t} = \alpha(x)\frac{\partial^2 u}{\partial x^2} + \beta(x)\frac{\partial u}{\partial x} + \gamma(x)u(x,t) + f(x,t) \tag{4.1}$$

$$u(a,t) = L(t) \tag{4.2}$$

$$u(b,t) = R(t) \tag{4.3}$$

$$u(x,0) = \phi(x) \tag{4.4}$$

These equations are solved numerically on a grid with N points and a constant step size h. Such a grid is called an equidistant grid. If the interval will be $[a,b]$, then the step size is equal to $h = (b-a)/N$. Let each point $a+ih$ be denoted by x_i.

4.1.1 Second order accuracy

To get a second order central difference approximation of the solution at point $x_i = a+ih$, Taylor expansions of the solution in the adjacent points are needed. Applying Taylor's expansions in the points $x_{i\pm1}$ gives:

$$\begin{aligned} u(x_{i\pm1}) = u_{x_i} \pm h\frac{\partial u}{\partial x}|_{x_i} + \frac{1}{2}h^2\frac{\partial^2 u}{\partial x^2}|_{x_i} \pm \frac{1}{6}h^3\frac{\partial^3 u}{\partial x^3}|_{x_i} + \\ + \frac{1}{24}h^4\frac{\partial^4 u}{\partial x^4}|_{x_i} \pm \frac{1}{120}h^5\frac{\partial^5 u}{\partial x^5}|_{x_i} + \mathbf{O}(h^6) \end{aligned}, \tag{4.5}$$

assuming that all relevant derivatives occurring exist. With linear combinations of u at point x_j, it is easily possible to get second order approximations of the first and second derivatives:

$$\frac{1}{h^2}\left(u_{i+1} - 2u_i + u_{i-1}\right) = \frac{\partial^2 u}{\partial x^2}|x_i + \mathbf{O}(h^2) \tag{4.6}$$

$$\frac{1}{2h}\left(u_{i+1} - u_{i-1}\right) = \frac{\partial u}{\partial x}|x_i + \mathbf{O}(h^2). \tag{4.7}$$

Here, u_i is the abbreviation for $u(x_i)$. It is then possible to discretize the differential equation (4.1). The factors in front of the differential operator can be evaluated in each point x_i. For the second order approximation, the semi-discretized systems turn into:

$$\frac{\partial u_i}{\partial t} = \alpha_i\frac{u_{i+1} - 2u_i + u_{i-1}}{h^2} + \beta_i\frac{u_{i+1} - u_{i-1}}{2h} + \gamma_i u_i + f_i(t) \tag{4.8}$$

These equations hold for $1 \leq i \leq N-1$. The first and last point of the system need special treatment. System of equations (4.8) reads in matrix form

$$\frac{d\mathbf{u}}{dt} = \mathbf{A}\mathbf{u} + \mathbf{b}(t) + \mathbf{f}(t) \tag{4.9}$$

with $\mathbf{f}$ is the discretized source function, $\mathbf{A}$ the coefficient matrix and $\mathbf{u}$ the discrete solution. The vector $\mathbf{b}$ contains the boundary values and may be a time-dependent function. The equation of the first point in second order accuracy reads:

$$\frac{\partial u_1}{\partial t} = \alpha_1\frac{u_2 - 2u_1 + u_0}{h^2} + \beta_i\frac{u_2 - u_0}{2h} + \gamma_1 u_1 + f_1(t) \tag{4.10}$$

with $u_0 = L(t)$ (4.2). In the same way, for the right boundary in second order:

$$\frac{\partial u_{N-1}}{\partial t} = \alpha_{N-1}\frac{u_N - 2u_{N-1} + u_{N-2}}{h^2} + \beta_{N-1}\frac{u_N - u_{N-2}}{2h} + \gamma_{N-1}u_{N-1} + f_{N-1}(t) \tag{4.11}$$

with $u_N = R(t)$. Vector $\mathbf{b}$ reads

$$b_i = \begin{cases} \left(\dfrac{\alpha(a+h)}{h^2} - \dfrac{\beta(a+h)}{2h}\right) L(t) & i = 1 \\ 0 & 2 \le i \le N-2 \\ \left(\dfrac{\alpha(b-h)}{h^2} + \dfrac{\beta(b-h)}{2h}\right) R(t) & i = N-1 \end{cases} \tag{4.12}$$

and the matrix elements read:

$$\begin{aligned} a_{ii} &= -\frac{2}{h^2}\alpha_i + \gamma_i \\ a_{ii+1} &= \frac{1}{h^2}\alpha_i + \frac{1}{2h}\beta_i \\ a_{ii-1} &= \frac{1}{h^2}\alpha_i - \frac{1}{2h}\beta_i. \end{aligned} \tag{4.13}$$

4.1.2 Fourth order accuracy

To get a fourth order accurate discretization, Taylor's expansion in more neighbouring points are needed. In the same way as (4.5) it follows for the points $x_{i\pm2}$:

$$\begin{aligned} u(x_{i\pm2}) = u_{x_i} \pm 2h\frac{\partial u}{\partial x}|_{x_i} + 2h^2\frac{\partial^2 u}{\partial x^2}|_{x_i} \pm \frac{4}{3}h^3\frac{\partial^3 u}{\partial x^3}|_{x_i}| + \\ + \frac{2}{3}h^4\frac{\partial^4 u}{\partial x^4}|_{x_i} \pm \frac{4}{15}h^5\frac{\partial^5 u}{\partial x^5}|_{x_i} + \mathbf{O}(h^6) \end{aligned} \tag{4.14}$$

Again assuming that all relevant derivatives exist. The fourth order approximations of the derivatives are therefore (with the same abbreviation $u_i = u(x_i)$):

$$\frac{1}{12h^2}\left(-u_{i+2} + 16u_{i+1} - 30u_i + 16u_{i-1} - u_{i-2}\right) = \frac{\partial^2 u}{\partial x^2}|x_i + \mathbf{O}(h^4) \tag{4.15}$$

$$\frac{1}{12h}\left(-u_{i+2} + 8u_{i+1} - 8u_{i-1} + u_{i-2}\right) = \frac{\partial u}{\partial x}|x_i + \mathbf{O}(h^4) \tag{4.16}$$

Combining (4.15) and (4.16), it follows that

$$\begin{aligned} \frac{\partial u_i}{\partial t} = \frac{1}{12h^2}\alpha_i\left(-u_{i+2} + 16u_{i+1} - 30u_i + 16u_{i-1} - u_{i-2}\right) + \\ + \frac{1}{12h}\beta_i\left(-u_{i+2} + 8u_{i+1} - 8u_{i-1} + u_{i-2}\right) + \gamma_i u_i + f_i(t) \end{aligned} \tag{4.17}$$

For the fourth order approximation, points x_1 and x_2 need special treatment at the left boundary and points x_{N-1} and x_{N-2} at the right boundary.

The equation of the system at the point x_2 is:

$$\begin{aligned}\frac{\partial u_2}{\partial t} &= \frac{1}{12h^2}\alpha_2\left(-u_4+16u_3-30u_2+16u_1-u_0\right)+\\ &+\frac{1}{12h}\beta_2\left(-u_4+8u_3-8u_1+u_0\right)+\gamma_2 u_2+f_2(t)\end{aligned} \tag{4.18}$$

And at the point x_1:

$$\begin{aligned}\frac{\partial u_1}{\partial t} &= \frac{1}{12h^2}\alpha_2\left(-u_3+16u_2-30u_1+16u_0-u_{-1}\right)+\\ &+\frac{1}{12h}\beta_2\left(-u_3+8u_2-8u_0+u_{-1}\right)+\gamma_1 u_1+f_1(t)\end{aligned} \tag{4.19}$$

Ghost value u_{-1} can be obtained by extrapolation. Different possibilities are

$$u_{-1} = 2u_0 - u_1 + \mathbf{O}(h^2) \tag{4.20}$$
$$u_{-1} = 3u_0 - 3u_1 + u_2 + \mathbf{O}(h^3) \tag{4.21}$$
$$u_{-1} = 4u_0 - 6u_1 + 4u_2 - u_3 + \mathbf{O}(h^4) \tag{4.22}$$
$$u_{-1} = 5u_0 - 10u_1 + 10u_2 - 5u_3 + u_4 + \mathbf{O}(h^5) \tag{4.23}$$

For the right boundary, the points x_{N-2} and x_{N-1} go similarly and therefore the derivation is omitted here.

Here, not only vector $\mathbf{b}$ changes, but also the first and last row of the matrix will change. Vector $\mathbf{b}$ as mentioned in (4.9) reads with the use of (4.22)

$$b_i = \begin{cases} \left(\dfrac{\alpha(a+h)}{h^2}-\dfrac{\beta(a+h)}{3h}\right)L(t) & i=1\\ \left(-\dfrac{\alpha(a+2h)}{12h^2}+\dfrac{\beta(a+2h)}{12h}\right)L(t) & i=2\\ 0 & 3\le i\le N-3\\ \left(\dfrac{-\alpha(b-2h)}{12h^2}-\dfrac{\beta(b-2h)}{12h}\right)R(t) & i=N-2\\ \left(\dfrac{\alpha(b-h)}{h^2}+\dfrac{\beta(b-h)}{3h}\right)R(t) & i=N-1 \end{cases} \tag{4.24}$$

And the matrix elements of (4.9) read

$$\begin{aligned} a_{ii} &= -\frac{15}{4h^2}\alpha_i + \gamma_i \\ a_{ii+1} &= \frac{4}{3h^2}\alpha_i + \frac{4}{h}\beta_i \\ a_{ii-1} &= \frac{4}{3h^2}\alpha_i - \frac{4}{h}\beta_i \\ a_{ii+2} &= -\frac{1}{12h^2}\alpha_i - \frac{1}{12h}\beta_i \\ a_{ii-2} &= -\frac{1}{12h^2}\alpha_i + \frac{1}{12h}\beta_i \end{aligned} \tag{4.25}$$

The corrected first and last row from (4.25) give

$$\begin{aligned} a_{11} &= -\frac{2}{h^2}\alpha(a+h) - \frac{1}{2h}\beta(a+h) + \gamma(a+h) \\ a_{12} &= \frac{1}{h^2}\alpha(a+h) + \frac{1}{h}\beta(a+h) \\ a_{13} &= -\frac{1}{6h}\beta(a+h) \\ a_{N-1,N-1} &= -\frac{2}{h^2}\alpha(b-h) + \frac{1}{2h}\beta(b-h) + \gamma(b-h) \\ a_{N-1,N-2} &= \frac{1}{h^2}\alpha(b-h) - \frac{1}{h}\beta(b-h) \\ a_{N-1,N-3} &= \frac{1}{6h}\beta(b-h) \end{aligned} \tag{4.26}$$

A second approach for the first and last grid point is to use backward differences at the first and last grid points, with difference scheme:

$$\frac{\partial u_1}{\partial x} = \frac{-3u_0 - 10u_1 + 18u_2 - 6u_3 + u_4}{12h^2} + \mathbf{O}(h^4) \tag{4.27}$$

$$\frac{\partial^2 u_1}{\partial x^2} = \frac{10u_0 - 15u_1 - 4u_2 + 14u_3 - 6u_4 + u_5}{12h^2} + \mathbf{O}(h^4) \tag{4.28}$$

and similarly for the last point:

$$\frac{\partial u_{N-1}}{\partial x} = \frac{3u_N + 10u_{N-1} - 18u_{N-2} + 6u_{N-3} - u_{N-4}}{12h^2} + \mathbf{O}(h^4) \tag{4.29}$$

$$\frac{\partial^2 u_{N-1}}{\partial x^2} = \frac{10u_N - 15u_{N-1} - 4u_{N-2} + 14u_{N-3} - 6u_{N-4} + u_{N-5}}{12h^2} + \mathbf{O}(h^4) \tag{4.30}$$

The corrected first and last row in (4.25) are now:

$$\begin{aligned}
a_{11} &= -\frac{5}{4h^2}\alpha(a+h) - \frac{5}{6h}\beta(a+h) + \gamma(a+h) \\
a_{12} &= -\frac{1}{3h^2}\alpha(a+h) + \frac{3}{2h}\beta(a+h) \\
a_{13} &= \frac{7}{6h^2}\alpha(a+h) - \frac{1}{2h}\beta(a+h) \\
a_{14} &= -\frac{1}{2h^2}\alpha(a+h) + \frac{1}{12h}\beta(a+h) \\
a_{15} &= \frac{1}{12h^2}\alpha(a+h) \\
a_{N-1,N-1} &= -\frac{5}{4h^2}\alpha(b-h) + \frac{5}{6h}\beta(b-h) + \gamma(b-h) \\
a_{N-1,N-2} &= -\frac{1}{3h^2}\alpha(b-h) - \frac{31}{2h}\beta(b-h) \\
a_{N-1,N-3} &= \frac{7}{6h^2}\alpha(a+h) - \frac{1}{2h}\beta(b-h) \\
a_{N-1,N-4} &= -\frac{1}{2h^2}\alpha(a+h) - \frac{1}{2h}\beta(b-h) \\
a_{N-1,N-5} &= \frac{1}{12h^2}\alpha(a+h)
\end{aligned} \tag{4.31}$$

The vector $\mathbf{b}$ only changes on the first and last element, so these elements in the vector $\mathbf{b}$ (4.24) read

$$\begin{aligned}
b_1 &= \left(\frac{5}{6h^2}\alpha(a+h) - \frac{1}{4h}\beta(a+h)\right) L(t) \\
b_{N-1} &= \left(\frac{5}{6h^2}\alpha(a+h) + \frac{1}{4h}\beta(b-h)\right) R(t)
\end{aligned} \tag{4.32}$$

4.2 Coordinate transformation

From [18] it follows that local grid refinement may give improved accuracy near singularities such as domain singularities (sharp corners) or singularities in the right hand side of an equation or in boundary or initial/final conditions. The finite difference approximation depends on the existence of many derivatives in the Taylor expansion, but in option pricing the final condition is typically not differentiable or even discontinuous. Therefore, local grid refinement near the non-differentiable or discontinuous payoff condition seems a logical choice to retain a satisfactory accuracy. The principle of local refinement is simple: Get more points in the neighbourhood of the grid point where the non differentiable condition occurs. This can be done by *adaptive* grid refinement for some regions, based

on an error indicator, or by a *coordinate transformation*, which results in an a-priori grid stretching. The latter is computationally more efficient if the region of interest for refinement is known beforehand. Adaptive grid refinement requires extra computations during the solution process to estimate the error, for example. An *analytic* coordinate transformation is the most elegant way in our applications. However, by the transformation the differential equation changes. The derived space discretization in section 4.1 is based on equidistant grid. This discretization can still be used after the analytic transformation, as only the coefficients in front of the derivatives change. Consider a coordinate transformation $y = \psi(x)$, which must be one-to-one, with inverse $x = \varphi(y) = \psi^{-1}(y)$. By the chain rule the first order derivative of a function $u(x)$ will be:

$$\frac{du}{dx} = \frac{du}{dy}\frac{dy}{dx} = \frac{du}{dy}\left(\frac{dx}{dy}\right)^{-1} = \frac{1}{\varphi'(y)}\frac{du}{dy} \tag{4.33}$$

By using (4.33), the second derivative reads

$$\begin{aligned}\frac{d^2u}{dx^2} &= \left(\frac{dx}{dy}\right)^{-1}\frac{d}{dy}\left(\left(\frac{dx}{dy}\right)^{-1}\frac{du}{dy}\right)\\ &= \left(\frac{dx}{dy}\right)^{-2}\frac{d^2u}{dy^2} - \left(\frac{dx}{dy}\right)^{-3}\frac{d^2x}{dy^2}\frac{du}{dy}\\ &= \frac{1}{(\varphi'(y))^2}\frac{d^2u}{dy^2} - \frac{\varphi''(y)}{(\varphi'(y))^3}\frac{du}{dy}\end{aligned} \tag{4.34}$$

Applying (4.33) and (4.34) to (4.1) changes the factors α, β and γ into:

$$\widehat{\alpha}(y) = \frac{\alpha(\varphi(y))}{(\varphi'(y))^2} \tag{4.35}$$

$$\widehat{\beta}(y) = \frac{\beta(\varphi(y))}{\varphi'(y)} - \alpha(\varphi(y))\frac{\varphi''(y)}{(\varphi'(y))^3} \tag{4.36}$$

$$\widehat{\gamma}(y) = \gamma(\varphi(y)) \tag{4.37}$$

Note that if $\beta = 0$ in the original equation, the transformed equation will contain an extra convection term. A standard diffusion equation turns into a convection-diffusion equation with non-constant coefficients.
The transformed equation is the target PDE to solve on an equidistant grid. The left and right boundary conditions are also transformed into $\psi(a)$ and $\psi(b)$. Our new step size for the transformed equation will be: $h_{new} = \dfrac{\psi(b) - \psi(a)}{N}$, assuming that the function ψ is a monotonically increasing function.

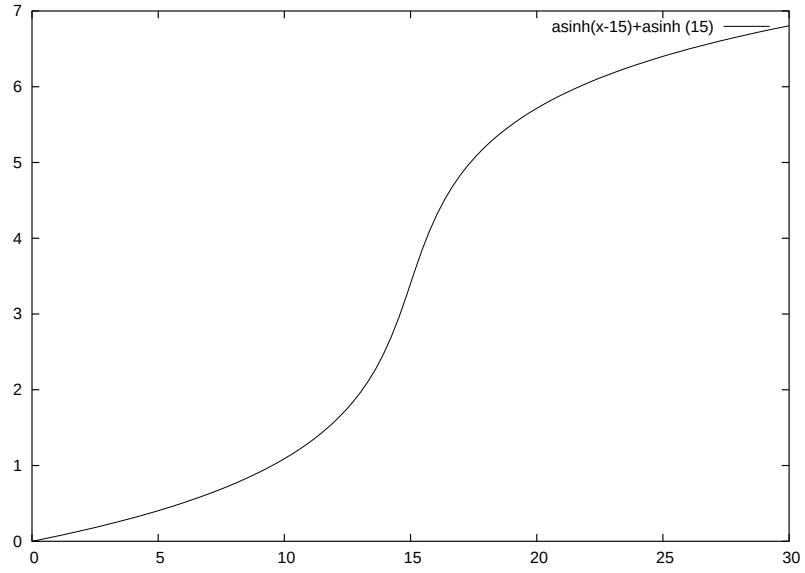

Figure 4.1: Transformation function (4.38).

4.2.1 Type of transformation

It is convenient to use a monotonically increasing function for the transformation. An interesting transformation for option pricing (see [6]) is:

$$y = \psi(S) = \sinh^{-1}(S - S_0) + \sinh^{-1} S_0 \tag{4.38}$$

Where $\sinh^{-1}$ is de inverse of sinh. Figure 4.1 depicts (4.38) for $S_0 = 15$. With a simple modification, it is possible to focus the local refinement at a specific point, for example at the exercise price ($S_0 = E$). The transformation used in this thesis reads:

$$y = \psi(S) = \sinh^{-1}\left(\mu\left(S - S_0\right)\right) + \sinh^{-1}\left(\mu S_0\right) \tag{4.39}$$

Parameter μ determines the rate of stretching. A satisfactory value in many cases is $\mu = 5$. With this equation, the grid is refined around $S = S_0$. Figure 4.2 shows the stretching function for $\mu = 1, 5, 10$. For example, the solution of a European call (3.15), with exercise price $E =$€ 15 and stretched around E has been plotted in figure 4.3

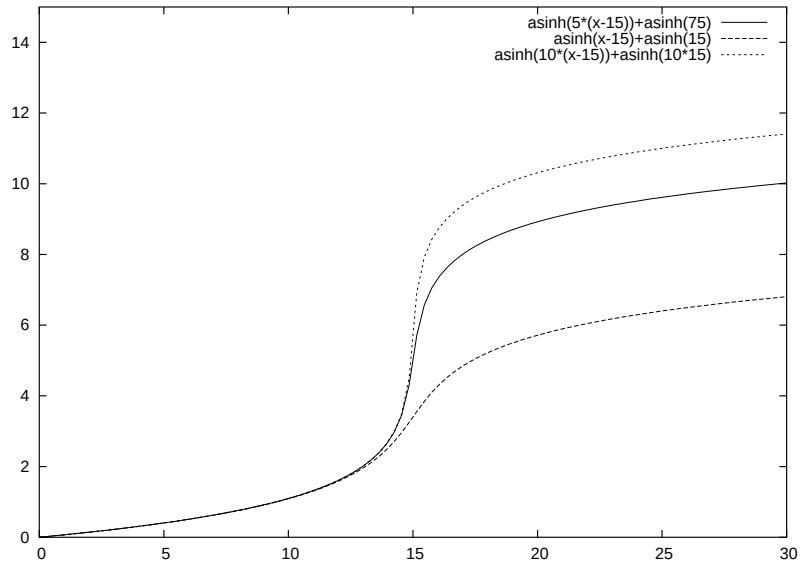

Figure 4.2: Transformation function (4.39) for $\mu = 1, 5, 10$.

For the transformation (4.39), the inverse and the derivatives are:

$$\varphi(y) = \frac{1}{\mu} \sinh\left(y - \sinh^{-1}\left(\mu S_0\right)\right) + S_0 \tag{4.40}$$

$$\varphi'(y) = \frac{1}{\mu} \cosh\left(y - \sinh^{-1}\left(\mu S_0\right)\right) \tag{4.41}$$

$$\varphi''(y) = \frac{1}{\mu} \sinh\left(y - \sinh^{-1}\left(\mu S_0\right)\right) \tag{4.42}$$

This transformation can also be applied at more points, say $x_1 \dots x_n$ if stretching around more than one point is needed. The transformation then becomes a sequence and can be written as one function

$$\begin{array}{ll} y = \psi_1(x) & z = \psi_2(y) \Leftrightarrow z = \psi_2(\psi_1(x)) \\ x = \varphi_1(y) & y = \varphi_2(z) \Leftrightarrow x = \varphi_1(\varphi_2(z)) \end{array} \tag{4.43}$$

4.3 Numerical time integration

After the space discretization of the equation, which may have been transformed, a system of ordinary differential equations remains.

$$\begin{cases} \dfrac{d\mathbf{u}}{dt} & = \mathbf{A}\mathbf{u} + \mathbf{b}(t) + \mathbf{f}(t) \\ \mathbf{u}(0) & = \phi \end{cases} \tag{4.44}$$

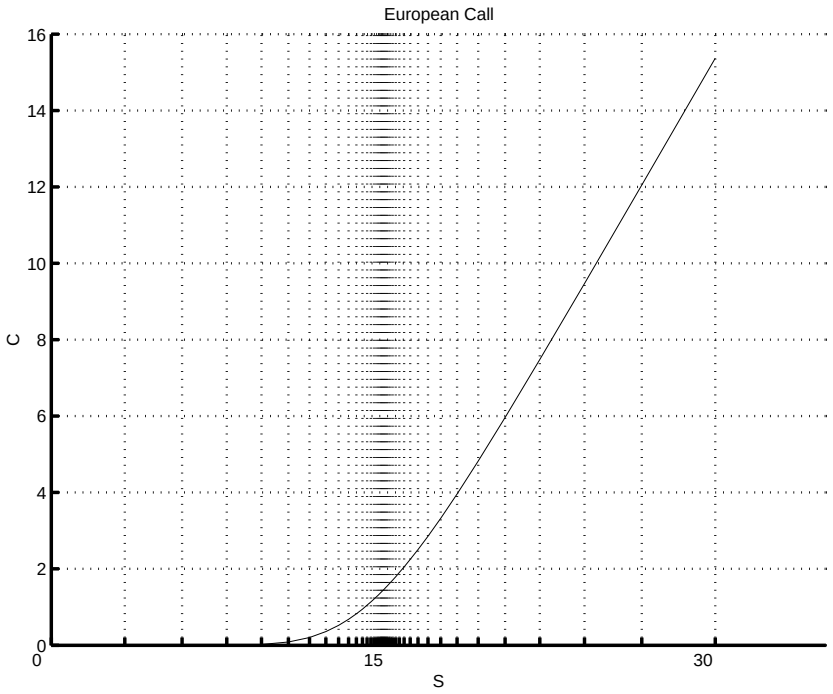

Figure 4.3: Solution of the Black-Scholes equation with a stretched grid

with $\mathbf{A}$ the matrix generated by the second or the fourth order scheme, the vector $\mathbf{b}$ contains boundary conditions. $\mathbf{f}(t)$ is the source function and ϕ the (transformed) initial condition (4.4). It is known, for example from [8], that pdes of diffusion type are stiff and we have to use implicit methods to solve them. We also employ a second or fourth order accurate scheme in time. Divide the time interval in M intervals and define the time step $k = \frac{T}{M}$. To get a second ($\mathbf{O}(h^2 + k^2)$) or fourth ($\mathbf{O}(h^4 + k^4)$) order approximation of the solution, a time integration of $\mathbf{O}(k^2)$ or $\mathbf{O}(k^4)$ is mandatory.

4.3.1 Crank Nicolson method

One of the most commonly used second order methods is the Crank-Nicolson scheme, see [4]. The scheme reads:

$$\left(\mathbf{I} - \frac{1}{2}k\mathbf{A}\right)\mathbf{u}^{j+1} = \left(\mathbf{I} + \frac{1}{2}k\mathbf{A}\right)\mathbf{u}^{j} + \frac{1}{2}k\left(\mathbf{b}^{j} + \mathbf{b}^{j+1} + \mathbf{f}^{j} + \mathbf{f}^{j+1}\right) \tag{4.45}$$

with $\mathbf{I}$ the identity matrix and $\mathbf{u}^j$ the vector evaluated at time $t = jk$. For non-smooth final conditions, the Crank-Nicolson is not satisfactory [15], because the method is not L-stable [8]. Numerical oscillations are not damped and remain to some extent. This may

also occur due to a discontinuous final condition. Therefore special damping initialization steps are necessary.

4.3.2 Backward difference methods

Another well-known implicit scheme is the backward difference scheme, BDF2 which is also $\mathbf{O}(k^2)$ (see [7]).

$$\left(\frac{3}{2}\mathbf{I} - k\mathbf{A}\right)\mathbf{u}^{j+1} = 2\mathbf{u}^j - \frac{1}{2}\mathbf{u}^{j-1} + k\left(\mathbf{b}^{j+1} + \mathbf{f}^{j+1}\right) \tag{4.46}$$

This method is a two-step method, which implies that an initialization step is necessary. Section 4.3.5 describes appropriate initialization steps.
The fourth order scheme reads

$$\left(\frac{25}{12}\mathbf{I} - k\mathbf{A}\right)\mathbf{u}^{j+1} = 4\mathbf{u}^j - 3\mathbf{u}^{j-1} + \frac{4}{3}\mathbf{u}^{j-2} + \frac{1}{4}\mathbf{u}^{j-3} + k\left(\mathbf{b}^{j+1} + \mathbf{f}^{j+1}\right) \tag{4.47}$$

This method needs three initialization steps.

4.3.3 Implicit Runge-Kutta methods

The fourth order method described in the previous section is a multi-step method. Runge-Kutta methods are one step but *multi-stage* methods, which means that more calculations are performed for one time step, but all of them with explicitly known time values. The most commonly used Runge-Kutta methods are based on Simpson's integration [8]. As mentioned above, we have to use an implicit method, because the scheme is stiff. The differential equation (4.44) can be rewritten into:

$$\mathbf{u}' = \mathbf{z}(t, \mathbf{u}) \tag{4.48}$$

$$\mathbf{u}(0) = \mathbf{u}_0 = \phi_0 \tag{4.49}$$

The general Runge-Kutta scheme can be given by (see [5]):

$$\begin{aligned} \mathbf{y}_\ell &= \mathbf{u}^j + k\sum_{m=1}^{q} p_{\ell m}\mathbf{z}(t^j + c_m k, \mathbf{y}_m) \\ \mathbf{u}^{j+1} &= \mathbf{u}^j + k\sum_{m=1}^{q} \omega_m \mathbf{z}(t^j + c_m k, \mathbf{y}_m) \end{aligned} \tag{4.50}$$

Because $p_{ii} \neq 0$, the total system is implicit and we have to solve a system of q equations with q unknown vectors of size $N-1$. But, if necessary , we can apply a LU-decomposition to tackle this problem. There are many different Runge-Kutta schemes described by the

so-called Butcher's array. The Runge-Kutta method used in this thesis is the $\mathbf{O}(k^4)$ Gauss-Legendre scheme. Its parameters are:

$$\begin{aligned} \mathbf{P} &= \begin{pmatrix} \frac{1}{4} & \frac{1}{4} - \frac{1}{6}\sqrt{3} \\ \frac{1}{4} + \frac{1}{6}\sqrt{3} & \frac{1}{4} \end{pmatrix} \\ \mathbf{c} &= \begin{pmatrix} \frac{1}{2} - \frac{1}{6}\sqrt{3} & \frac{1}{2} + \frac{1}{6}\sqrt{3} \end{pmatrix}^T \\ \omega &= \begin{pmatrix} \frac{1}{2} & \frac{1}{2} \end{pmatrix}^T \end{aligned} \tag{4.51}$$

4.3.4 Padé methods

Another multi-stage, one step difference formula for ordinary differential equations in the form (4.48) is given by the Padé methods (see [8]). The so-called Padé(1,1) method reads

$$\mathbf{u}^{j+1} = \mathbf{u}^j + \frac{1}{2}k\left(\mathbf{A}\mathbf{u}^j + \mathbf{b}^j + \mathbf{f}^j + \mathbf{A}\mathbf{u}^{j+1} + \mathbf{b}^{j+1} + \mathbf{f}^{j+1}\right) + \mathbf{O}(k^2) \tag{4.52}$$

This scheme is the well-known Crank Nicolson scheme. The scheme of Padé(1,2) is

$$\begin{aligned} \mathbf{u}^{j+1} = \mathbf{u}^j &+ \frac{1}{3}k\left(\mathbf{A}\mathbf{u}^j + \mathbf{b}^j + \mathbf{f}^j\right) + \frac{2}{3}k\left(\mathbf{A}\mathbf{u}^{j+1} + \mathbf{b}^{j+1} + \mathbf{f}^{j+1}\right) + \\ &- \frac{1}{6}k^2\left(\mathbf{A}\left(\mathbf{A}\mathbf{u}^{j+1} + \mathbf{b}^{j+1} + \mathbf{f}^{j+1}\right) + \frac{d\mathbf{b}^{\mathbf{j+1}}}{dt} + \frac{d\mathbf{f}^{\mathbf{j+1}}}{dt}\right) + \mathbf{O}(k^3) \end{aligned} \tag{4.53}$$

and the scheme Padé(2,2) reads

$$\begin{aligned} \mathbf{u}^{j+1} = \mathbf{u}^j &+ \frac{1}{2}k\left(\mathbf{A}\mathbf{u}^j + \mathbf{b}^j + \mathbf{f}^j + \mathbf{A}\mathbf{u}^{j+1} + \mathbf{b}^{j+1} + \mathbf{f}^{j+1}\right) + \\ &+ \frac{1}{12}k^2\left(\mathbf{A}\left(\mathbf{A}\mathbf{u}^j + \mathbf{b}^j + \mathbf{f}^j\right) + \frac{d\mathbf{b}^{\mathbf{j}}}{dt} + \frac{d\mathbf{f}^{\mathbf{j}}}{dt}\right) + \\ &- \frac{1}{12}k^2\left(\mathbf{A}\left(\mathbf{A}\mathbf{u}^{j+1} + \mathbf{b}^{j+1} + \mathbf{f}^{j+1}\right) + \frac{d\mathbf{b}^{\mathbf{j+1}}}{dt} + \frac{d\mathbf{f}^{\mathbf{j+1}}}{dt}\right) + \mathbf{O}(k^4) \end{aligned} \tag{4.54}$$

The derivatives of vector $\mathbf{b}$ and the source vector $\mathbf{f}$ can easily be calculated. All these methods are implicit due to the fact that on both sides $\mathbf{u}^{j+1}$ appears.

4.3.5 Initialization

For the second order approach, an initialization step is needed for the $BDF2$ method (4.46). This can be done by taking one step of the Crank Nicolson method (4.45). Non-smooth initial conditions must sometimes be treated by another initialization step, which

exhibits damping. For that purpose, two steps of the Backward Euler scheme (first order) can be applied, see [14]:

$$(\mathbf{I} - k\mathbf{A})\,\mathbf{u}^{j+1} = \mathbf{u}^{j} + k\left(\mathbf{b}^{j+1} + \mathbf{f}^{j+1}\right). \tag{4.55}$$

For the fourth order time integration, several possibilities for the initialization of BDF4 can be given. The Padé and Runge-Kutta methods are both one step methods, but they are complicated, due to the multi-staging. For the Runge-Kutta method, matrix equations have to be inverted. They cost substantial CPU time. With the Padé approximation, both matrix multiplications as well as matrix inversions have to be performed. An elegant way is to combine fourth order methods described in the previous sections as follows. Take four steps of the Gauss Legendre method (4.51) and continue with BDF 4 (4.47). Padé could also be used as an initialization for the BDF 4 method. Another approach is to start with the BDF 2 scheme continued by the BDF 3 scheme and finally continue with the BDF 4 method. The BDF 3 method is given by:

$$\left(\frac{11}{6}\mathbf{I} - k\mathbf{A}\right)\mathbf{u}^{j+1} = 3\mathbf{u}^{j} - \frac{3}{2}\mathbf{u}^{j-1} + \frac{1}{3}\mathbf{u}^{j-3} + k\left(\mathbf{b}^{j+1} + \mathbf{f}^{j+1}\right) \tag{4.56}$$

In this thesis, the combination of Backward Euler (4.55) and Crank Nicolson (4.45) is used for the second order solution and the combination of Runge-Kutta (4.50) and (4.51) with BDF4 (4.47) is used for fourth order solutions. The other methods are alternatives, but for this thesis the methods chosen are to be preferred.

4.4 Numerical differentiation: the Greeks

As mentioned in section 3.4, the Greeks are calculated by numerical differentiation. It is done by using the different schemes for discretization of the Black-Scholes equation. Given the solution of the problem $u(x_i, t)$, then the derivatives with a second order accurate scheme read:

$$\Delta_i = \frac{\partial u}{\partial x} = \frac{u_{i+1} - u_{i-1}}{2h} \tag{4.57}$$

$$\Gamma_i = \frac{\partial^2 u}{\partial x^2} = \frac{u_{i+1} - 2u_i + u_{i-1}}{h^2}, \tag{4.58}$$

and for the fourth order accurate scheme

$$\Delta_i = \frac{\partial u}{\partial x} = \frac{-u_{i+2} + 8u_{i+1} - 8u_{i-1} + u_{i-2}}{12h} \tag{4.59}$$

$$\Gamma_i = \frac{\partial^2 u}{\partial x^2} = \frac{-u_{i+2} + 16u_{i+1} - 30u_i + 16u_{i-1} - u_{i-2}}{12h^2}. \tag{4.60}$$

The derivatives at the boundaries are known for Black-Scholes, but with the fourth order accurate scheme, one needs the backward differences to find the derivatives in the points u_1 and u_{N-1}. The derivatives read in those points:

$$\Delta_1 = \frac{\partial u}{\partial x} = \frac{-3u_0 - 10u_1 + 18u_2 - 6u_3 + u_4}{12h} \tag{4.61}$$

$$\Gamma_1 = \frac{\partial^2 u}{\partial x^2} = \frac{10u_0 - 15u_1 - 4u_2 + 14u_3 - 6u_4 + u_5}{12h^2} \tag{4.62}$$

$$\Delta_{N-1} = \frac{\partial u}{\partial x} = \frac{3u_N + 10u_{N-1} - 18u_{N-2} + 6u_{N-3} - u_{N-4}}{12h} \tag{4.63}$$

$$\Gamma_{N-1} = \frac{\partial^2 u}{\partial x^2} = \frac{10u_N - 15u_{N-1} - 4u_{N-2} + 14u_{N-3} - 6u_{N-4} + u_{N-5}}{12h^2}. \tag{4.64}$$

If the transformation is used, the same schemes can be employed, but now the derivatives read:

$$\Delta_{T,i} = \frac{d\varphi}{dy}_i \Delta_i \tag{4.65}$$

$$\Gamma_{T,i} = \left(\frac{d\varphi}{dy}\right)_i^{-2} \Gamma_i - \frac{d^2\varphi}{dy^2}\left(\frac{d\varphi}{dy}\right)_i^{-3} \Delta_i \tag{4.66}$$

The derivatives of the transformation are also known in each point.

Chapter 5

Validation of the discrete systems

Before applying the discretizations derived in chapter 4 to the Black Scholes equation, some reference tests are performed with diffusion type equations and with an analytic solution in the form of a polynomial. The fourth order scheme is tested. The numerical error can be given in the maximum norm $\|\cdot\|_\infty$ or in the $\mathbf{L}^2$-norm:

$$\epsilon_\infty = \|\mathbf{u} - \mathbf{u}_{ex}\|_\infty = \max\{|u_i - u_{ex,i}| : i = 1 \cdots N\} \tag{5.1}$$

$$\epsilon_2 = \|\mathbf{u} - \mathbf{u}_{ex}\|_2 = \frac{1}{N}\sqrt{\sum_{i=1}^{N} (u_i - u_{ex,i})^2} \tag{5.2}$$

where, $\mathbf{u}$ is the numerical solution and $\mathbf{u}_{ex}$ is the exact solution. Note that $|u_i - u_{ex,i}|$ is the error made at point $x_i = a + ih$. In the Black Scholes equation, the value a will be set to zero, and all calculations are performed in the interval $[0, b]$

5.1 Test problem with constant coefficients

The first problem to test the fourth order discretization in space and time is a parabolic partial differential equation with constant coefficients

$$\begin{aligned} \frac{\partial u}{\partial t} &= \frac{1}{2}\frac{\partial^2 u}{\partial x^2} + \frac{\partial u}{\partial x} - u(x,t) + f(x,t) \\ u(0,t) &= -t^5 \\ u(b,t) &= (b-t)^5 \\ u(x,0) &= x^5 \\ f(x,t) &= (x-t)^5 - 10(x-t)^4 - 10(x-t)^3 \end{aligned} \tag{5.3}$$

The exact solution is given by:

$$u(x,t) = (x-t)^5 \tag{5.4}$$

For the solution where $T = 1$, $b = 1$, $N = 10$ space and $M = 10$ time steps with *extrapolation at the boundaries*, the matrix of (5.3) reads:

$$\begin{pmatrix} -106 & 60 & -1.67 & 0 & 0 & 0 & 0 & 0 & 0 \\ 60 & -126 & 73.33 & -5 & 0 & 0 & 0 & 0 & 0 \\ -3.33 & 60 & -126 & 73.33 & -5 & 0 & 0 & 0 & 0 \\ 0 & -3.33 & 60 & -126 & 73.33 & -5 & 0 & 0 & 0 \\ 0 & 0 & -3.33 & 60 & -126 & 73.33 & -5 & 0 & 0 \\ 0 & 0 & 0 & -3.33 & 60 & -126 & 73.33 & -5 & 0 \\ 0 & 0 & 0 & 0 & -3.33 & 60 & -126 & 73.33 & -5 \\ 0 & 0 & 0 & 0 & 0 & -3.33 & 60 & -126 & 73.33 \\ 0 & 0 & 0 & 0 & 0 & 0 & 1.67 & 40 & -96 \end{pmatrix}$$

Typical for the fourth order space discretization is the pentadiagonal structure of the matrix. In table 5.1 a test with different numbers of space and time steps is performed for (5.3). The errors and the order of convergence in both infinity norm as well as in $\mathbf{L}^2$ norm are presented.

Grid	$\|u - u_{ex}\|_\infty$	$\|u - u_{ex}\|_2$	Conv_∞	Conv_2
10×10	8.05×10^{-4}		5.49×10^{-4}	
20×20	5.91×10^{-5}	13.64	3.79×10^{-5}	14.47
40×40	4.06×10^{-6}	14.56	2.50×10^{-6}	15.16
80×80	2.67×10^{-7}	15.19	1.61×10^{-7}	15.54

Table 5.1: Results of test problem (5.3) with $b = 1, T = 1$ and extrapolation at the boundaries

The matrix changes when applying *backward differences* at the boundaries in the first and last row:

$$\begin{pmatrix} -71.83 & -1.67 & 53.33 & -24.17 & 4.17 & 0 & 0 & 0 & 0 \\ 60 & -126 & 73.33 & -5 & 0 & 0 & 0 & 0 & 0 \\ -3.33 & 60 & -126 & 73.33 & -5 & 0 & 0 & 0 & 0 \\ 0 & -3.33 & 60 & -126 & 73.33 & -5 & 0 & 0 & 0 \\ 0 & 0 & -3.33 & 60 & -126 & 73.33 & -5 & 0 & 0 \\ 0 & 0 & 0 & -3.33 & 60 & -126 & 73.33 & -5 & 0 \\ 0 & 0 & 0 & 0 & -3.33 & 60 & -126 & 73.33 & -5 \\ 0 & 0 & 0 & 0 & 0 & -3.33 & 60 & -126 & 73.33 \\ 0 & 0 & 0 & 0 & 4.17 & -25.83 & 63.33 & -31.67 & -55.17 \end{pmatrix}$$

The same results with the errors and the convergence is given in table 5.2. Asymptotically, fourth order accuracy is observed in both tables. The error with backward differences at the boundaries is smaller than that with extrapolation.

5.2 Test problem with non-constant coefficients

The Black Scholes equation has non-constant coefficients, so also a test has been performed with the following parabolic equation.

$$\begin{aligned} \frac{\partial u}{\partial t} &= \frac{1}{2}x^2\frac{\partial^2 u}{\partial x^2} + x\frac{\partial u}{\partial x} - u(x,t) + f(x,t) \\ u(0,t) &= -t^5 \\ u(b,t) &= (b-t)^5 \\ u(x,0) &= x^5 \\ f(x,t) &= (x-t)^5 - 5(x-t)^4 - 5x(x-t)^4 - 10x^2(x-t)^3 \end{aligned} \tag{5.5}$$

The solution is also given by:

$$u(x,t) = (x-t)^5$$

In table 5.3 the errors and the order of convergence in both the infinity norm as well as in the $\mathbf{L}^2$ norm are presented with backward differences at the boundaries. The convergence behaviour is again asymptotically of fourth order. The errors are somewhat larger than for the previous equation.

5.3 Transformed test problem

The same test problem (5.5) has been investigated, but now with the grid transformation described in section 4.2.
The matrix for $N = 10$ space and $M = 10$ time steps with $b = 1$, $T = 1$, $\mu = 5$, $x_0 = 0.5$

Grid	$\|u - u_{ex}\|_\infty$	Conv_∞	$\|u - u_{ex}\|_2$	Conv_2
10×10	5.20×10^{-4}		3.59×10^{-4}	
20×20	3.42×10^{-5}	15.19	2.43×10^{-5}	14.77
40×40	2.16×10^{-6}	15.82	1.56×10^{-6}	15.63
80×80	1.35×10^{-7}	15.96	9.82×10^{-8}	15.85

Table 5.2: Results of test problem (5.3) with $b = 1, T = 1$ and backward differences at the boundary points

and extrapolation at boundaries reads

$$\begin{pmatrix} -3.03 & 2.03 & -0.23 & 0 & 0 & 0 & 0 & 0 & 0 \\ 2.37 & -9.88 & 7.10 & -0.59 & 0 & 0 & 0 & 0 & 0 \\ -0.30 & 8.94 & -25.66 & 17.36 & -1.35 & 0 & 0 & 0 & 0 \\ 0 & -0.93 & 20.36 & -49.50 & 31.38 & -2.31 & 0 & 0 & 0 \\ 0 & 0 & -1.77 & 33.33 & -72.98 & 43.45 & -3.03 & 0 & 0 \\ 0 & 0 & 0 & -2.38 & 41.27 & -84.23 & 47.50 & -3.16 & 0 \\ 0 & 0 & 0 & 0 & -2.47 & 40.82 & -79.96 & 43.40 & -2.79 \\ 0 & 0 & 0 & 0 & 0 & -2.14 & 34.66 & -66.85 & 35.58 \\ 0 & 0 & 0 & 0 & 0 & 0 & 0.09 & 20.08 & -41.96 \end{pmatrix}$$

The matrix for $N = 10$ space and $M = 10$ time steps with $b = 1$, $T = 1$,$\mu = 5$, $x_0 = 0.5$ and backward differencing at the boundaries reads:

$$\begin{pmatrix} -2.97 & 1.81 & 0.11 & -0.22 & 0.06 & 0 & 0 & 0 & 0 \\ 2.37 & -9.88 & 7.10 & -0.59 & 0 & 0 & 0 & 0 & 0 \\ -0.30 & 8.94 & -25.66 & 17.36 & -1.35 & 0 & 0 & 0 & 0 \\ 0 & -0.93 & 20.36 & -49.50 & 31.38 & -2.31 & 0 & 0 & 0 \\ 0 & 0 & -1.77 & 33.33 & -72.98 & 43.45 & -3.03 & 0 & 0 \\ 0 & 0 & 0 & -2.38 & 41.27 & -84.23 & 47.50 & -3.16 & 0 \\ 0 & 0 & 0 & 0 & -2.47 & 40.82 & -79.96 & 43.40 & -2.79 \\ 0 & 0 & 0 & 0 & 0 & -2.14 & 34.66 & -66.85 & 35.58 \\ 0 & 0 & 0 & 0 & 1.72 & -10.35 & 24.32 & -7.68 & -26.32 \end{pmatrix}$$

The errors and order of convergence are given in the tables 5.4-5.5.

With respect to convergence, we prefer backward differencing at the boundaries.

As a next test, we evaluate the influence of μ in our transformation. In the same test problem, we vary only μ and choose $\mu = 1$ and $\mu = 10$. The convergence results are presented in tables 5.6 and 5.7.

From the test experiments, it follows that the equidistant grid converges in fourth order, but with the transformed grid this is observed mainly asymptotically. The errors

Grid	$\|u - u_{ex}\|_\infty$	Conv_∞	$\|u - u_{ex}\|_2$	Conv_2
10×10	1.17×10^{-3}		7.97×10^{-4}	
20×20	8.58×10^{-5}	13.59	5.98×10^{-5}	13.32
40×40	5.71×10^{-6}	15.03	4.02×10^{-6}	14.86
80×80	3.67×10^{-7}	15.56	2.60×10^{-7}	15.46

Table 5.3: Results of test problem (5.5) with $b = 1, T = 1$ and backward differencing at boundaries

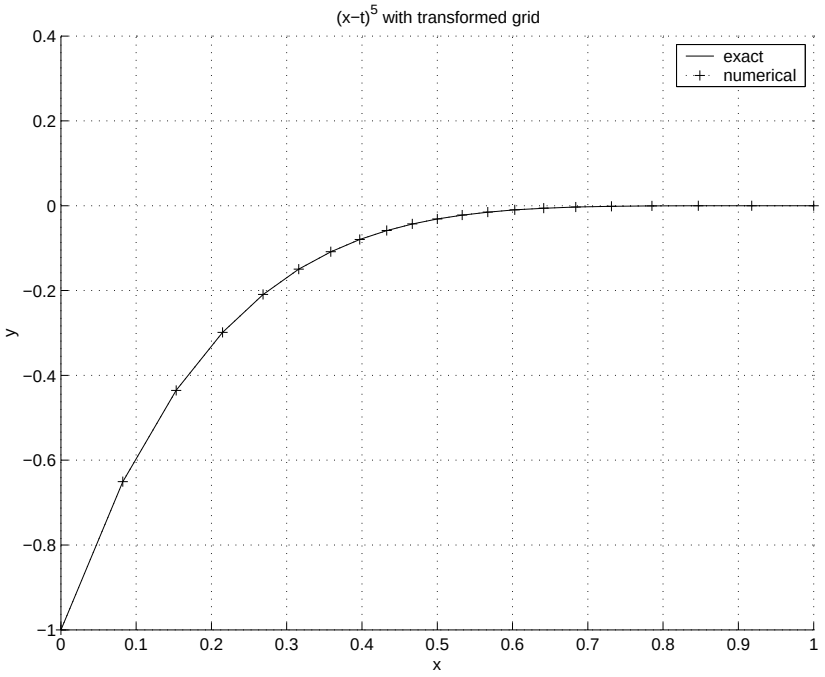

Figure 5.1: Solution of transformed test problem (5.5) with $\mu = 10$ and $x_0 = 0.5$

made, however, are lower when a proper μ has been chosen. For $\mu = 10$, the lower convergence with only a few grid points is probably due to the severe stretching: in the outer regions very few grid points are left, as can be seen in figure 5.1. For Black Scholes x_0 will often be chosen close to E and the parameter μ plays an important role for convergence and for the error. For the test problems discussed in this chapter, the transformation is not very useful, as a singularity does not occur. This will be different for the option pricing problems.

Grid	$\|u - u_{ex}\|_\infty$	Conv_∞	$\|u - u_{ex}\|_2$	Conv_2
10×10	5.48×10^{-4}		3.64×10^{-4}	
20×20	1.30×10^{-4}	4.21	9.09×10^{-5}	4.00
40×40	1.46×10^{-5}	8.88	1.04×10^{-5}	8.72
80×80	1.35×10^{-6}	10.81	8.69×10^{-7}	12.01

Table 5.4: Results of transformed test problem (5.5) with $b = 1, T = 1$ $\mu = 5$, $x_0 = 0.5$ and extrapolation at the boundaries

Grid	$\|u - u_{ex}\|_\infty$	Conv_∞	$\|u - u_{ex}\|_2$	Conv_2
10×10	1.51×10^{-3}		5.88×10^{-4}	
20×20	2.16×10^{-4}	6.97	8.47×10^{-5}	6.93
40×40	1.82×10^{-5}	11.86	8.16×10^{-6}	10.38
80×80	1.21×10^{-6}	15.01	6.10×10^{-7}	13.38

Table 5.5: Results of transformed test problem (5.5) with $b = 1, T = 1$ $\mu = 5$, $x_0 = 0.5$ and backward differences

Grid	$\|u - u_{ex}\|_\infty$	Conv_∞	$\|u - u_{ex}\|_2$	Conv_2
10×10	1.22×10^{-3}		7.99×10^{-4}	
20×20	9.18×10^{-5}	13.28	6.20×10^{-5}	12.90
40×40	6.12×10^{-6}	15.00	4.22×10^{-6}	14.66
80×80	3.92×10^{-7}	15.60	2.74×10^{-7}	15.41

Table 5.6: Results of transformed test problem (5.5) with $b = 1, T = 1$ $\mu = 1$, $x_0 = 0.5$ and backward differences

Grid	$\|u - u_{ex}\|_\infty$	Conv_∞	$\|u - u_{ex}\|_2$	Conv_2
10×10	1.45×10^{-3}		6.15×10^{-4}	
20×20	4.07×10^{-4}	3.55	1.27×10^{-4}	4.85
40×40	4.48×10^{-5}	9.09	1.51×10^{-5}	8.40
80×80	3.33×10^{-6}	13.47	1.31×10^{-6}	11.49

Table 5.7: Results of transformed test problem (5.5) with $b = 1, T = 1$ $\mu = 10$, $x_0 = 0.5$ and backward differences

Chapter 6

Special features of the Black Scholes PDE

In this chapter, some topics especially related to the Black Scholes equation will be discussed in order to choose the proper difference scheme, transformation and choice of grid. Three techniques to smooth the final condition will be discussed. These techniques include:

- Transformation of the grid
- Initializing steps in time integration
- Choice of grid with respect to the position of the non-differentiability.

The last section gives the procedure to the problem to find the so-called implied volatility.

6.1 Difference scheme and redefinition of time

Local refinement can be used near singularities, such as discontinuities in final conditions. First of all, the time direction is transformed to obtain a forward problem with an initial condition. The new time will be $\tau = T - t$. Applying this to (3.15), it follows that:

$$\begin{aligned} \frac{\partial C}{\partial \tau} &= \frac{1}{2}\sigma^2 S^2 \frac{\partial^2 C}{\partial S^2} + (r-\delta) S \frac{\partial C}{\partial S} - rC(S,\tau) \\ C(0,\tau) &= 0 \\ C(S,\tau) &= Se^{-\delta\tau} - Ee^{-r\tau} \\ C(S,0) &= \max(S-E,0) = \begin{cases} S-E & S > E \\ 0 & S < E \end{cases} \end{aligned} \tag{6.1}$$

This system is well-posed and can be solved by the numerical schemes described in chapter 4. From now on, τ will be replaced by t, for convenience. Applying the grid stretching transformation (4.39) to the initial condition, with $x_0 = E$ it follows that:

$$C(y,0) = \max\left(\frac{1}{\mu}\sinh(y - \sinh^{-1}\mu E), 0\right) \tag{6.2}$$

The sharp edge in the initial condition of a European option disappears, as shown in the left picture of figure 6.1. The right picture of figure 6.1 shows that a discontinuous payoff remains a discontinuity in the transformed case.

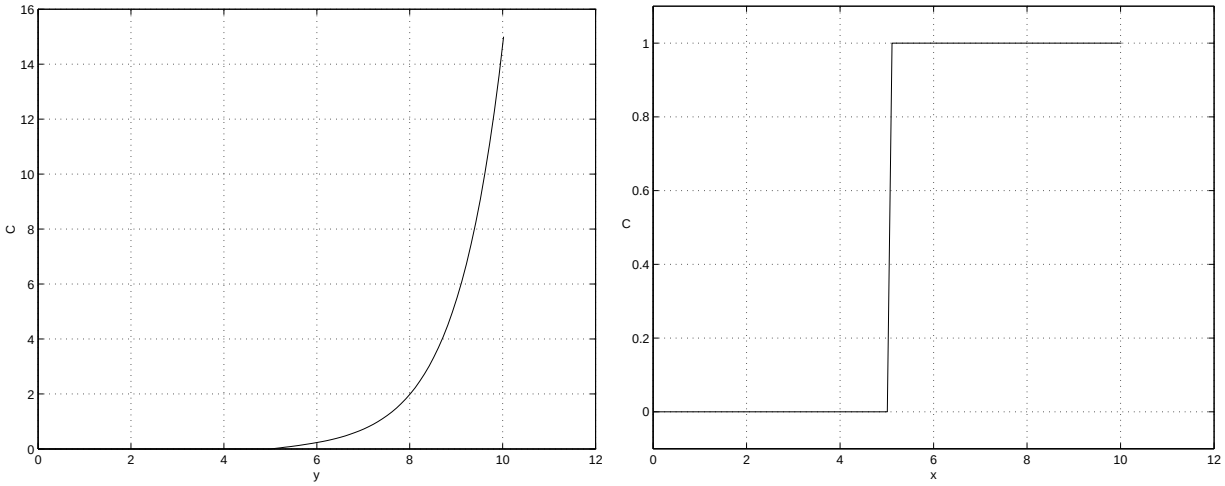

(a) Vanilla call

(b) Digital call

Figure 6.1: Transformation of the initial condition

6.2 Initial time steps

A discontinuous initial condition must be treated carefully when applying a time integration scheme. From [15], it follows that the initial condition has been smoothed by applying one or more first order time steps as initialization for Crank Nicolson. A possibility for initialization for the fourth order time scheme is to start with the Runge-Kutta method from section 4.3.3. We will use this also for the non-differentiable initial condition.

6.3 Far field boundary

The described numerical solution in chapter 4 deals with a fixed boundary, but in the case of Black Scholes there is a boundary condition at infinity. This means that S_{max} must be chosen "as large as possible". For a numerical scheme, this can be problematic as the number of grid points may grow tremendously. In [11] the proper size of the domain is proposed after a careful analysis. The *far field boundary* reads:

$$S_{max} = \max(2E, E \exp\left(\sqrt{2\sigma^2 T \ln 100}\right)) \tag{6.3}$$

Here a relation between S_{max} and E has been given, also σ plays an important role. With this formula, a solution can be computed with an accuracy of at least $E/100$. With (6.3) the minimal size of the domain is $2E$. However, in practical cases, brokers would like to have an accuracy of at least € 0,01, so in this thesis after some experiments, the following formula has been used:

$$S_{max} = \max(RE, E \exp\left(\sqrt{2\sigma^2 T \ln 100}\right) \tag{6.4}$$

This equation is also valid in the case that σ is very high. In that case $R > 2$ is necessary. In an equidistant grid, there would be many points without any financial interest (the region $S \in [2E, RE]$). Here the strength of the transformation comes up as the number of points in this region will be minimized (see figure 6.2). Only one point remains in the

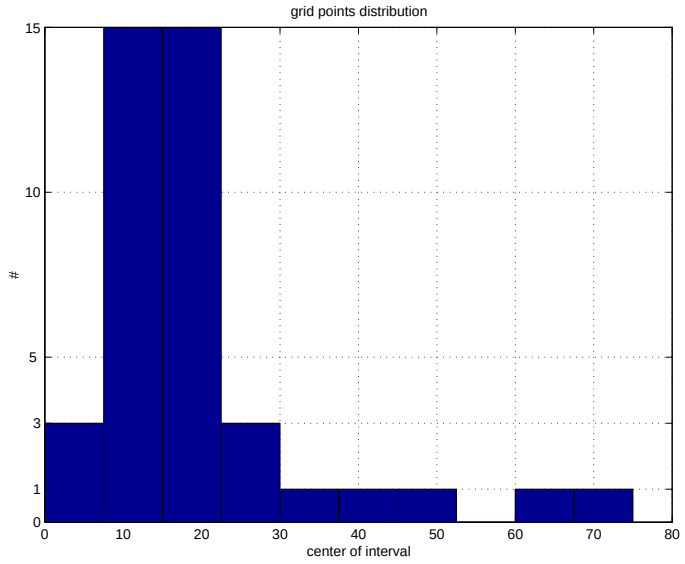

Figure 6.2: Number of points in the intervals, $E = 15, \mu = 5, N = 40$

outer regions, so the stretching is very useful for this purpose.

6.4 Choice of grid

From [14], it follows that the exact position of a *discontinuity* in the initial condition related to the position of the grid points is important for the accuracy. Test results in [14] show that if E is not exactly between two grid points when applying a numerical scheme to a digital option as described in (3.23), a satisfactory accuracy will not be obtained. Two algorithms can be applied to get E on the right position.

6.4.1 E on the grid

First of all, we propose a method to get E on a grid point after transformation. Assume that the maximal value of the grid will be related to E, according to (6.4), in the sense that $S_{max} = RE$, with $R \geq 2$ and assume a grid of N points. S_{max} must be translated to the right side, to satisfy to both properties, $S_{max} > RE$ and E on a grid point. In the equidistant grid, there are about N/R points on the left side of E and the others are at the right side of E. Since grid points have to be integer numbers, the floor function is used, which returns the lower integer ($\lfloor 2.235 \rfloor = 2$). The nearest neighbouring grid point to E will be given by:

$$\eta = \lfloor \frac{N}{R} \rfloor \tag{6.5}$$

Then the step size will be given by:

$$h = \frac{E}{\eta} \tag{6.6}$$

The new maximal value of the grid is then: $S_{max} = Nh$.
The transformation (4.39), which is not linear, requires another treatment. In case of the stretched grid, the property $S_{max} = RE$ transforms into $y_{max} = q\psi(E)$, with:

$$q = \frac{\psi(RE)}{\psi(E)} \tag{6.7}$$

then combining with (6.5), the nearest grid point reads:

$$\eta_T = \lfloor \frac{N}{q} \rfloor \tag{6.8}$$

and new step size will become:

$$h = \frac{\psi(E)}{\eta_T}. \tag{6.9}$$

6.4.2 E between two grid points

Only a slight modification in the definition of the step size is enough to get E in the middle between two grid points (say x_n and x_{n+1}). The points $E - \frac{1}{2}h$ and $E + \frac{1}{2}h$ are now on the grid, so with (6.5), it follows that:

$$h = \frac{E + \frac{1}{2}h}{\eta} \Leftrightarrow h = \frac{E}{\eta}\left(1 - \frac{1}{2\eta}\right)^{-1}. \tag{6.10}$$

And with transformations and (6.8) we find:

$$h = \frac{\psi(E) + \frac{1}{2}h}{\eta_T} \Leftrightarrow h = \frac{\psi(E)}{\eta_T}\left(1 - \frac{1}{2\eta_T}\right)^{-1} \tag{6.11}$$

6.5 Lagrange interpolation

With the transformation, many points are in the region around E, but sometimes values in the neighbourhood of E must be calculated which are not on the grid. A typical example is that option values are required near the present asset price S_0. An appropriate way is the Lagrange interpolation. The interpolation polynomial for calculating the point x given the set $[x_i : i = 1 \cdots n]$ and $x \neq x_i : \forall i$ is given by:

$$P(x) = \sum_{j=1}^{n} x_j \prod_{\substack{j=1 \\ j \neq k}}^{n} \frac{x - x_k}{x_j - x_k} \tag{6.12}$$

For a second order interpolation, only two points $x \in [x_1, x_2]$ are necessary

$$P(x) = x_1 \frac{x - x_2}{x_1 - x_2} + x_2 \frac{x - x_1}{x_2 - x_1}, \tag{6.13}$$

and for fourth order, four points are necessary ($x \in [x_0, x_4]$).

$$\begin{aligned} P(x) = x_1 &\frac{x - x_2}{x_1 - x_2}\frac{x - x_3}{x_1 - x_3}\frac{x - x_4}{x_1 - x_4} + \\ + x_2 &\frac{x - x_1}{x_2 - x_1}\frac{x - x_3}{x_2 - x_3}\frac{x - x_4}{x_2 - x_4} + \\ + x_3 &\frac{x - x_1}{x_3 - x_1}\frac{x - x_2}{x_3 - x_2}\frac{x - x_4}{x_3 - x_4} + \\ + x_4 &\frac{x - x_1}{x_4 - x_1}\frac{x - x_2}{x_4 - x_2}\frac{x - x_3}{x_4 - x_3} \end{aligned} \tag{6.14}$$

These formulae can simply be applied to the unknown value $y(x)$. These procedures are necessary in volatility search. If there is only one point to the left of a certain point, then three points at the other side should be taken.

6.6 Implied volatility

How is it is possible to estimate or predict the volatility? The difficult part is that σ is sensitive to the behaviour of the market in the future. Two important types of volatility are: implied and historical volatility.

If we have an option for six months and we have all the parameters of the same option from half a year earlier, then we could use the known information to calculate the historical volatility. As all the parameters are known, we can calculate the profit of our option half a year later. This can be a basis for a prediction of the future volatility. The volatility is, however, a stochastic value and if the asset price S changes, so does the volatility.

Suppose we would like to know the market expectation of the volatility of the underlying asset for a six month option. With the price of this option from the newspaper, it is possible to calculate the volatility underlying these option prices assumed by the traders. Indeed, we know the strike price E, today's value of the underlying asset denoted by S_0, and most important of all, we know the price of our benchmark option, V. Then using Black-Scholes formulae (see chapter 3) we get: $V = \mathcal{L}_{BS}(S, t, T, r, \sigma, E)$, where V is the known option price. Finding σ from uit expression is an implicit problem. The σ obtained when solving this equation is called the "implied volatility". Implied volatility is then based on today's market and not on yesterday's values. Finding σ is an implicit problem. It can be obtained with the help of root finding methods.

Volatility search is in some sense solving an *inverse* problem. Two basic techniques to find the volatility will be discussed: the interval bisection method (Golden search) and the inverse quadratic interpolation method.

6.6.1 The bisection method

The procedure to find the solution σ_{imp} is as follows (see [12]).

1. Take two values of σ: σ_{high} and σ_{low} in such the way that if $C_{market} = C(\sigma_{imp})$ then $C(\sigma_{imp}) < C(\sigma_{high})$ and $C(\sigma_{imp}) > C(\sigma_{low})$ due to the monotonicity of $C(\sigma)$, we can setup a root finding procedure. It is trivial that $\sigma_{imp} \in (\sigma_{low}, \sigma_{high})$.

2. Take $\sigma_{mid} = \frac{1}{2}(\sigma_{low} + \sigma_{high})$

3. Calculate $C(\sigma_{mid})$

4. Calculate $Q = (C_{market} - C(\sigma_{mid})) \times (C_{market} - C(\sigma_{high}))$.

5. If $Q < 0$ then $\sigma_{low} = \sigma_{mid}$, otherwise, if $Q > 0$ then $\sigma_{high} = \sigma_{mid}$ and repeat from 2 until the desired accuracy is reached.

This procedure is known to be very robust, but it is a slowly converging method for practical applications.

6.6.2 Inverse quadratic interpolation method

Consider the solution of the general Black-Scholes equation as a function of σ and subtract the known market price, $V(\sigma) - V_{market}$ (V_{market} follows from the newspaper). $V(\sigma)$ is a nonlinear function and a derivative (for general options) is generally not known. The inverse quadratic interpolation procedure to determine σ is as follows [9]:

1. Choose three σ's, called σ_a, σ_b and σ_c
2. Calculate $V_a = V(\sigma_a) - V_{market}$, $V_b = V(\sigma_b) - V_{market}$ and $V_c = V(\sigma_c) - V_{market}$
3. Define $u = \dfrac{V_b}{V_c}$, $v = \dfrac{V_b}{V_a}$ and $w = \dfrac{V_a}{V_c}$
4. Define $p = v(w(u-w)(\sigma_c - \sigma_b) - (1-u)(\sigma_b - \sigma_a))$ and $q = (u-1)(v-1)(w-1)$.
5. Then: $\sigma_c = \sigma_a$, $\sigma_a = \sigma_b$, $\sigma_b = \sigma_b + \dfrac{p}{q}$ and $V_c = V_a$, $V_a = V_b$ and compute the new iterant $V_b = V(\sigma_b) - V_{market}$
6. If $|V_b| < \varepsilon$ then $\sigma_{market} = \sigma_b$. Otherwise repeat from 3

The advantage is that only one calculation of the option price must be done. The convergence is known to be "almost" quadratically [9].

Chapter 7

Numerical option pricing experiments

The numerical experiments performed in this chapter are related to the option pricing problems described in chapter 3 and the volatility search explained in section 6.6. In all cases the value of an option is computed with parameters:

$$\begin{aligned} E &= 15 \\ \sigma &= 30\ \% \\ r &= 4\ \% \\ \delta &= 2\ \% \\ T &= 0.5 \quad \text{half a year} \end{aligned}$$

If other parameters are tested, this is explicitly mentioned.

7.1 European vanilla options

The European (vanilla) call is useful as a basic reference option. Many properties of the numerical schemes can be investigated, as an analytic solution is available. From the test results in chapter 5, the backward difference scheme will be used at the boundaries, because the accuracy is better than with extrapolation. In all computations the numerical solution is compared to the analytic solution. This defines the error in the following tables.

7.1.1 Equidistant grids

First of all, we show that the second order accurate scheme in space and time (based on Crank Nicolson), results in second order accuracy for our reference option. This computation is performed on the equidistant grid. In table 7.1 and 7.2 two test results

are given. The first one is on an equidistant grid with S_{max} from equation (6.3). The second one is a test where E is placed exactly between two grid points.

Grid	$\|C - C_{ex}\|_\infty$	Conv_∞	$\|\Delta - \Delta_{ex}\|_\infty$	Conv_∞	$\|\Gamma - \Gamma_{ex}\|_\infty$	Conv_∞
10×10	1.68×10^{-1}		3.03×10^{-2}		3.22×10^{-2}	
20×20	3.55×10^{-2}	4.73	1.01×10^{-2}	2.99	6.19×10^{-3}	5.21
40×40	8.57×10^{-3}	4.15	2.78×10^{-3}	3.64	1.55×10^{-3}	3.98
80×80	2.13×10^{-3}	4.02	7.05×10^{-4}	3.95	3.80×10^{-4}	4.09

Table 7.1: Crank Nicolson solution of the European call with S_{max} as in (6.4) with $R = 2$

Grid	$\|C - C_{ex}\|_\infty$	Conv_∞	$\|\Delta - \Delta_{ex}\|_\infty$	Conv_∞	$\|\Gamma - \Gamma_{ex}\|_\infty$	Conv_∞
10×10	4.46×10^{-2}		1.53×10^{-2}		2.12×10^{-3}	
20×20	1.10×10^{-2}	4.04	2.95×10^{-3}	5.19	3.13×10^{-3}	0.68
40×40	2.60×10^{-3}	4.24	8.07×10^{-4}	3.65	7.82×10^{-4}	4.01
80×80	6.33×10^{-4}	4.11	2.47×10^{-4}	3.27	1.91×10^{-4}	4.09

Table 7.2: Crank Nicolson solution of a call with E between two grid points as in section 6.3.2 with $R = 2$

In table 7.2 there appears to be some loss of convergence. However applying equation (6.4) with $R = 3$, it follows from table 7.3 that the convergence is retained. The convergence is again second order, because we have chosen the outer boundary far enough. In mathematical analysis, the asymptotic convergence plays an important role. There-

Grid	$\|C - C_{ex}\|_\infty$	Conv_∞	$\|\Delta - \Delta_{ex}\|_\infty$	Conv_∞	$\|\Gamma - \Gamma_{ex}\|_\infty$	Conv_∞
10×10	1.33×10^{-1}		9.74×10^{-2}		2.13×10^{-2}	
20×20	3.31×10^{-2}	4.02	9.60×10^{-3}	10.14	6.22×10^{-3}	3.42
40×40	6.38×10^{-3}	5.18	1.73×10^{-3}	5.55	1.88×10^{-3}	3.30
80×80	1.53×10^{-3}	4.18	4.94×10^{-4}	3.50	4.59×10^{-4}	4.10

Table 7.3: Crank Nicolson solution of a call with E between two grid points as in section 6.3.2, now with $R = 3$

fore the results in table 7.3 are to be preferred. The parameter R in equation (6.4) is important.

The matrix of the discrete system is:

$$\begin{pmatrix} -0.14 & 0.06 & 0 & 0 & 0 & 0 & 0 & 0 & 0 \\ 0.16 & -0.41 & 0.20 & 0 & 0 & 0 & 0 & 0 & 0 \\ 0 & 0.38 & -0.86 & 0.44 & 0 & 0 & 0 & 0 & 0 \\ 0 & 0 & 0.68 & -1.49 & 0.76 & 0 & 0 & 0 & 0 \\ 0 & 0 & 0 & 1.08 & -2.30 & 1.18 & 0 & 0 & 0 \\ 0 & 0 & 0 & 0 & 1.56 & -3.29 & 1.68 & 0 & 0 \\ 0 & 0 & 0 & 0 & 0 & 2.14 & -4.46 & 2.27 & 0 \\ 0 & 0 & 0 & 0 & 0 & 0 & 2.80 & -5.81 & 2.96 \\ 0 & 0 & 0 & 0 & 0 & 0 & 0 & 3.56 & -7.34 \end{pmatrix}$$

This matrix is diagonally dominant. Iterative methods, like the Gauss-Seidel method could be applied to the second order discretization. The matrix is the same for all values of S_{max} and h, because the element are not proportional to these parameters, but only to i, which is the number of the grid point. In table 7.4, the error and the convergence of error are shown at the point of non-differentiability $S = E$. The accuracy is better, if the scheme is applied with E between two grid points.

Grid	error in E E on a grid point	Conv_∞	error in E E between two points	Conv_∞
10×10	1.68×10^{-1}		4.32×10^{-2}	
20×20	3.55×10^{-2}	4.73	1.94×10^{-3}	22.31
40×40	8.57×10^{-3}	4.15	1.87×10^{-4}	10.34
80×80	2.13×10^{-3}	4.03	3.12×10^{-5}	6.02

Table 7.4: Crank Nicolson solution of a call at the point $S = E$, with $R = 2$ in (6.4)

In table 7.5 and 7.6 the convergence with the fourth order scheme has been displayed, once with E on a grid points and once with E between two grid points. Immediately, it follows that a fourth order approximation has not been achieved on an equidistant grid. Both tests use equation (6.4) with $R = 3$. The accuracy obtained is not higher than with the second order scheme on the equidistant grids.

Grid	$\|C - C_{ex}\|_\infty$	Conv_∞	$\|\Delta - \Delta_{ex}\|_\infty$	Conv_∞	$\|\Gamma - \Gamma_{ex}\|_\infty$	Conv_∞
10×10	3.30×10^{-1}		3.72×10^{-2}		2.27×10^{-2}	
20×20	7.46×10^{-2}	4.42	1.15×10^{-2}	3.22	1.06×10^{-2}	2.14
40×40	1.39×10^{-2}	5.35	3.04×10^{-3}	3.80	1.49×10^{-3}	7.11
80×80	3.41×10^{-3}	4.09	7.88×10^{-4}	3.86	3.58×10^{-4}	4.15

Table 7.5: Fourth order solution of the European call with E on a grid point

Grid	$\|C - C_{ex}\|_\infty$	Conv_∞	$\|\Delta - \Delta_{ex}\|_\infty$	Conv_∞	$\|\Gamma - \Gamma_{ex}\|_\infty$	Conv_∞
10×10	1.60×10^{-1}		9.51×10^{-2}		2.23×10^{-2}	
20×20	3.70×10^{-2}	4.32	1.71×10^{-2}	5.57	3.65×10^{-3}	6.12
40×40	7.12×10^{-3}	5.19	2.01×10^{-3}	8.48	6.45×10^{-4}	5.66
80×80	1.75×10^{-3}	4.07	4.34×10^{-4}	4.64	1.74×10^{-4}	3.70

Table 7.6: Fourth order solution of the European call with E between two grid points

7.1.2 Transformed grid

In this section only the fourth order scheme will be used. The second order scheme just remains second order accurate after transformation. The application of the transformation (4.39) with different values of μ will be given in tables 7.7 to 7.10. In these experiments, S_{max} is determined from (6.4) with $R = 3$. It is beforehand not determined where E is located. μ varies between 1, 2.5, 5 and 10.

Grid	$\|C - C_{ex}\|_\infty$	Conv_∞	$\|\Delta - \Delta_{ex}\|_\infty$	Conv_∞	$\|\Gamma - \Gamma_{ex}\|_\infty$	Conv_∞
10×10	1.05×10^{-2}		1.94×10^{-2}		6.30×10^{-3}	
20×20	1.05×10^{-3}	10.04	3.14×10^{-3}	6.16	1.32×10^{-3}	4.78
40×40	9.33×10^{-5}	11.24	2.92×10^{-4}	10.78	9.69×10^{-5}	13.61
80×80	2.52×10^{-5}	3.70	2.55×10^{-5}	11.42	8.89×10^{-6}	10.90

Table 7.7: Fourth order solution of the European call with $R = 3$ in (6.4) and $\mu = 1$

Grid	$\|C - C_{ex}\|_\infty$	Conv_∞	$\|\Delta - \Delta_{ex}\|_\infty$	Conv_∞	$\|\Gamma - \Gamma_{ex}\|_\infty$	Conv_∞
10×10	4.32×10^{-2}		4.40×10^{-2}		1.23×10^{-2}	
20×20	2.60×10^{-3}	16.60	5.68×10^{-3}	7.75	4.81×10^{-4}	25.61
40×40	2.04×10^{-4}	12.73	6.56×10^{-4}	8.65	2.31×10^{-4}	2.08
80×80	1.51×10^{-5}	13.49	5.13×10^{-5}	12.79	1.99×10^{-5}	11.58

Table 7.8: Fourth order solution of the European call with $R = 3$ in (6.4) and $\mu = 2.5$

Grid	$\|C - C_{ex}\|_\infty$	Conv_∞	$\|\Delta - \Delta_{ex}\|_\infty$	Conv_∞	$\|\Gamma - \Gamma_{ex}\|_\infty$	Conv_∞
10×10	1.08×10^{-1}		7.77×10^{-2}		2.67×10^{-2}	
20×20	6.44×10^{-3}	16.77	8.76×10^{-3}	8.86	2.75×10^{-3}	9.70
40×40	4.03×10^{-4}	15.96	8.49×10^{-4}	10.32	3.71×10^{-4}	7.42
80×80	2.79×10^{-5}	14.44	8.24×10^{-5}	10.30	3.34×10^{-5}	11.13

Table 7.9: Fourth order solution of the European call with $R = 3$ in (6.4) and $\mu = 5$

With only 20 points in space and time, a solution with an accuracy of one cent (€ 0.01) is achieved with the transformation ($\mu = 1, 2.5, 5$). This is a satisfactory result. In the next tests, we place E on a grid point (table 7.11) and exactly between two grid points (table 7.12) and choose $\mu = 5$.

It follows from these experiments that the position of the non-differentiability is not very important for the accuracy (This will be completely different for the digital option

Grid	$\|C - C_{ex}\|_\infty$	Conv_∞	$\|\Delta - \Delta_{ex}\|_\infty$	Conv_∞	$\|\Gamma - \Gamma_{ex}\|_\infty$	Conv_∞
10×10	2.28×10^{-1}		1.48×10^{-1}		3.92×10^{-2}	
20×20	1.28×10^{-2}	17.85	9.09×10^{-3}	16.25	4.20×10^{-3}	9.34
40×40	7.76×10^{-4}	16.44	1.56×10^{-3}	5.82	4.49×10^{-4}	9.36
80×80	4.90×10^{-5}	15.85	1.41×10^{-4}	11.03	4.00×10^{-5}	11.21

Table 7.10: Fourth order solution of the European call with $R = 3$ in (6.4) and $\mu = 10$

Grid	$\|C - C_{ex}\|_\infty$	Conv_∞	$\|\Delta - \Delta_{ex}\|_\infty$	Conv_∞	$\|\Gamma - \Gamma_{ex}\|_\infty$	Conv_∞
10×10	2.23×10^{-1}		1.38×10^{-1}		4.01×10^{-2}	
20×20	7.32×10^{-3}	30.42	8.82×10^{-3}	15.68	3.41×10^{-3}	11.78
40×40	4.33×10^{-4}	16.92	1.08×10^{-3}	8.17	3.72×10^{-4}	9.15
80×80	1.87×10^{-5}	23.11	8.89×10^{-5}	12.15	3.52×10^{-5}	10.58

Table 7.11: Fourth order solution of the European call with E on a grid point

with discontinuous final conditions). For completeness, table 7.13 presents the error and the convergence at the point $S = E$. With all three possibilities in table 7.13 only twenty grid points are sufficient for the required accuracy. The effect of the transformation is an increasing number of points in the region around $S = E$, influenced by the parameter μ. In figure 7.1 the distribution of points in the intervals is displayed. The higher μ, the fewer the number of points in the outer regions. All figures in 7.1 are done with the reference option except figure 7.1(d), which belongs to an option with $E = 150$. The stretched grid and the solution are displayed in figure 7.2. It follows that the fourth order scheme in combination with the transformation is preferred. The parameter μ is a stretching parameter, which has a big influence to the accuracy and the convergence of the solution. In the remaining of this chapter, all tests are done with the fourth order scheme and the transformation, with R from equation (6.4) and μ in the transformation will be adjusted to create the best solution. For example, options with large values of E or σ may need other values of μ. In tables 7.14-7.16, parameter E of the reference option has been changed between, 0.15, 1.5, 15 and 150. All test have been performed by using the equation (6.4) and, therefore, the grid position of E is not known. It can be seen from these tables, that for each E, the convergence is similar and the absolute value of the error increases with a factor 10 if E increases with a factor 10. In the transformation $\mu E = \text{constant}$ is satisfactory.

Grid	$\|C - C_{ex}\|_\infty$	Conv_∞	$\|\Delta - \Delta_{ex}\|_\infty$	Conv_∞	$\|\Gamma - \Gamma_{ex}\|_\infty$	Conv_∞
10×10	4.01×10^{-1}		2.62×10^{-1}		6.16×10^{-2}	
20×20	9.34×10^{-3}	42.99	7.68×10^{-3}	34.12	4.13×10^{-3}	14.91
40×40	5.34×10^{-4}	17.48	1.26×10^{-3}	6.10	3.43×10^{-4}	12.02
80×80	3.10×10^{-5}	17.22	9.75×10^{-5}	12.92	3.75×10^{-5}	9.15

Table 7.12: Fourth order solution of the European call with E between two points

Grid	error in E place E N.N.	Conv_∞	error in E E on a grid point	Conv_∞	error in E E between points	Conv_∞
10×10	8.47×10^{-2}		1.78×10^{-1}		3.27×10^{-1}	
20×20	5.10×10^{-3}	16.62	5.75×10^{-3}	31.04	7.44×10^{-3}	44.02
40×40	3.22×10^{-4}	15.83	3.36×10^{-4}	17.11	4.28×10^{-4}	17.40
80×80	2.29×10^{-5}	14.04	1.31×10^{-5}	25.71	2.55×10^{-5}	16.77

Table 7.13: Fourth order solution of a Call in the point $S = E$ ($\mu = 5$)

7.1.3 European Put

The basic insights and results obtained for the call option will also be valid for put options. Otherwise the put-call parity (3.22) will be violated. In table 7.17 the results of the test have been displayed. The test has been performed with the outer boundary determined by (6.4) and, therefore, the place of E is not known. Almost the same errors and convergence are obtained as in the test with the call options.

Grid	$\|C - C_{ex}\|_\infty$	Conv_∞	$\|\Delta - \Delta_{ex}\|_\infty$	Conv_∞	$\|\Gamma - \Gamma_{ex}\|_\infty$	Conv_∞
10×10	1.08×10^{-3}		7.77×10^{-2}		2.67	
20×20	6.44×10^{-5}	16.77	8.76×10^{-3}	8.86	2.75×10^{-1}	9.70
40×40	4.03×10^{-6}	15.96	8.49×10^{-4}	10.32	3.71×10^{-2}	7.42
80×80	2.79×10^{-7}	14.44	8.24×10^{-5}	10.30	3.34×10^{-3}	11.13

Table 7.14: European Call with $E = 0.15$, $\mu = 500$ and $R = 3$

Grid	$\|C - C_{ex}\|_\infty$	Conv_∞	$\|\Delta - \Delta_{ex}\|_\infty$	Conv_∞	$\|\Gamma - \Gamma_{ex}\|_\infty$	Conv_∞
10×10	1.08×10^{-2}		7.77×10^{-2}		2.67×10^{-1}	
20×20	6.44×10^{-4}	16.77	8.76×10^{-3}	8.86	2.75×10^{-2}	9.70
40×40	4.03×10^{-5}	15.96	8.49×10^{-4}	10.32	3.71×10^{-3}	7.42
80×80	2.79×10^{-6}	14.44	8.24×10^{-5}	10.30	3.34×10^{-4}	11.13

Table 7.15: European Call with $E = 1.5$, $\mu = 50$ and $R = 3$

Grid	$\|C - C_{ex}\|_\infty$	Conv_∞	$\|\Delta - \Delta_{ex}\|_\infty$	Conv_∞	$\|\Gamma - \Gamma_{ex}\|_\infty$	Conv_∞
10×10	1.08		7.77×10^{-2}		2.67×10^{-3}	
20×20	6.44×10^{-2}	16.77	8.76×10^{-3}	8.86	2.75×10^{-4}	9.70
40×40	4.03×10^{-3}	15.96	8.49×10^{-4}	10.32	3.71×10^{-5}	7.42
80×80	2.79×10^{-4}	14.44	8.24×10^{-5}	10.30	3.34×10^{-6}	11.13

Table 7.16: European Call with $E = 150$, $\mu = 0.5$ and $R = 3$

Grid	$\|P - P_{ex}\|_\infty$	Conv_∞	$\|\Delta - \Delta_{ex}\|_\infty$	Conv_∞	$\|\Gamma - \Gamma_{ex}\|_\infty$	Conv_∞
10×10	9.65×10^{-2}		8.35×10^{-2}		2.83×10^{-2}	
20×20	6.13×10^{-3}	15.74	8.69×10^{-3}	9.61	2.75×10^{-3}	10.32
40×40	3.95×10^{-4}	15.53	1.02×10^{-3}	8.50	3.42×10^{-4}	8.04
80×80	2.74×10^{-5}	14.42	9.40×10^{-5}	10.88	3.45×10^{-5}	9.89

Table 7.17: Solution of the European Put ($\mu = 5, R = 3$), parameters as in the reference option.

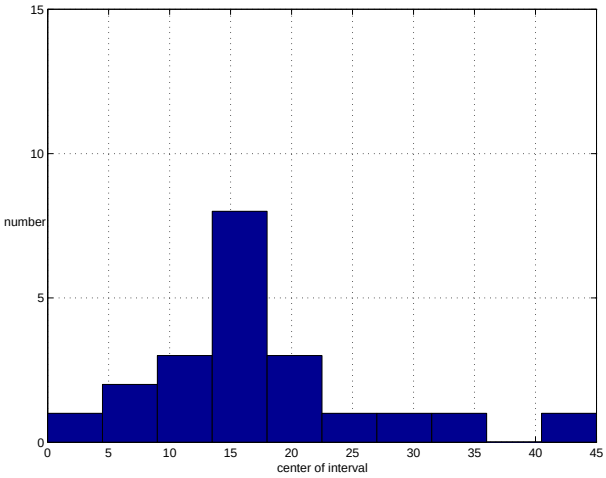

(a) $\mu = 1$

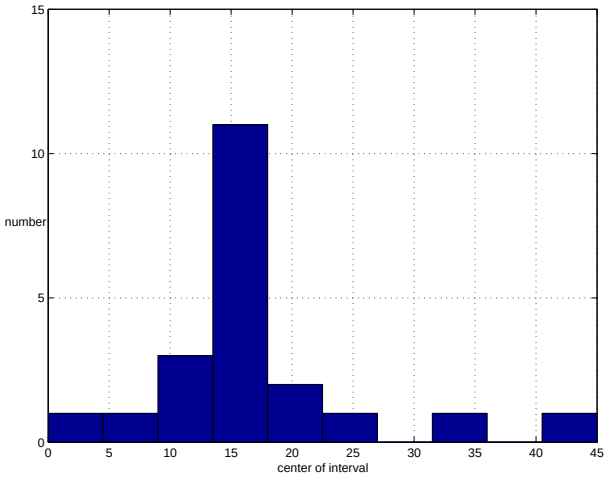

(b) $\mu = 5$

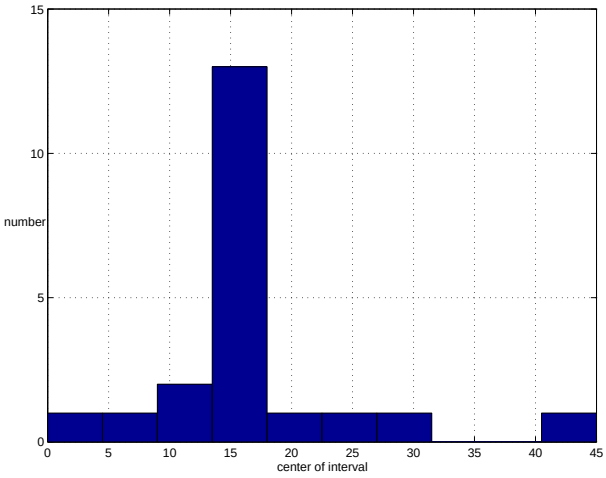

(c) $\mu = 10$

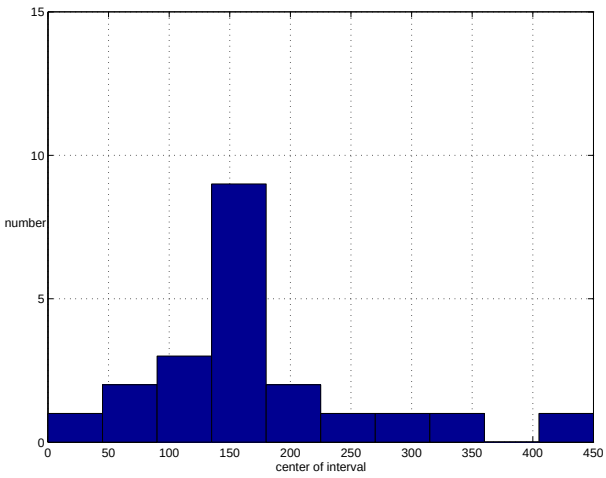

(d) $\mu = 0.2$,$E = 150$

Figure 7.1: Plots of distribution of points

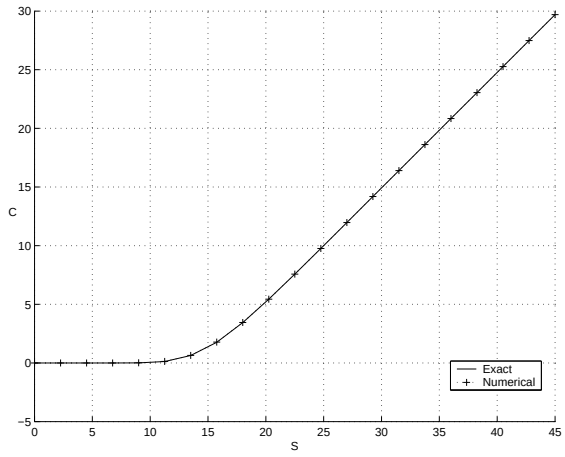

(a) Equidistant

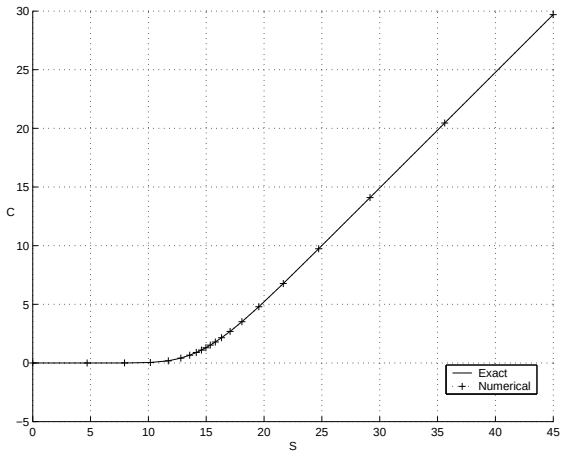

(b) $\mu = 1$

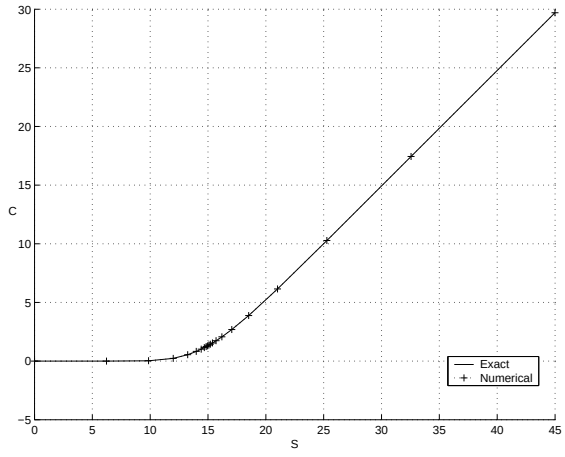

(c) $\mu = 5$

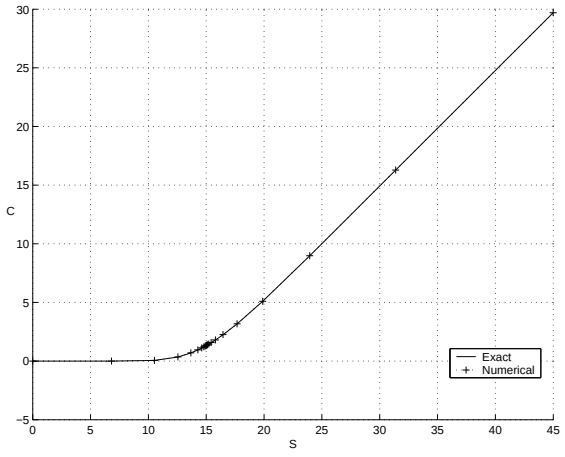

(d) $\mu = 10$

Figure 7.2: Plots of option price of a call with the stretched grids

7.2 Digital options

Specially for digital options with the discontinuous final conditions, we need a proper time integration. The Greeks are the parameters in which numerical oscillations may occur, with an improper numerical time integration. The lack of damping properties in the Crank Nicolson scheme is clearly seen in Γ, for example (see [14]). We confirm this computation with Crank Nicolson for $N = 100$ and $M = 10$. The parameters for this option are:

$$\begin{aligned} E &= 40 \\ \sigma &= 30\ \% \\ r &= 5\ \% \\ \delta &= 0\ \% \\ T &= \text{half a year} \end{aligned}$$

In figures 7.3 and 7.4, the solution of the option C and Γ of this option have been plotted. They are compared with the exact solution. The numerical solution presented are a pure Crank Nicolson discretization and secondly, the Crank Nicolson scheme preceded by two steps of backward Euler (equidistant grid, second order in space) and our fourth order discretization with BDF4 and grid stretching. Figure 7.4 shows that only the Crank Nicolson discretization gives numerical oscillations in hedge parameter Γ. All other results are very satisfactory.

Because of the discontinuous final condition, the position of E with respect to the grid is important for the accuracy of the numerical solution. Therefore, two tests will be performed; one with E on a grid point and one with E exactly between two points. The parameters are the same as for the previous test. We choose fewer points in space. μ is chosen such that $\mu E = 75$. The results are presented in tables 7.18 and 7.19. It can be

Grid	$\|C - C_{ex}\|_\infty$	Conv_∞	$\|\Delta - \Delta_{ex}\|_\infty$	Conv_∞	$\|\Gamma - \Gamma_{ex}\|_\infty$	Conv_∞
10×10	2.23×10^{-2}		9.40×10^{-3}		1.58×10^{-3}	
20×20	6.74×10^{-3}	3.31	1.40×10^{-3}	6.70	4.33×10^{-4}	3.65
40×40	3.39×10^{-3}	1.99	4.81×10^{-4}	2.91	5.54×10^{-5}	7.80
80×80	1.65×10^{-3}	2.05	1.51×10^{-4}	3.19	2.47×10^{-5}	2.24

Table 7.18: European digital call, E on a grid point $\mu = 1.875$

seen that the position of E with respect to the grid is very important for digital options. With our method and E between two grid points, we have asymptotically a fourth order accurate solution. With E on a grid point the accuracy reduces to first order only.

The next tests are therefore performed with E between two grid points of the stretched grid (see section 6.3.2). We present some results for other digital options. In table 7.20, for

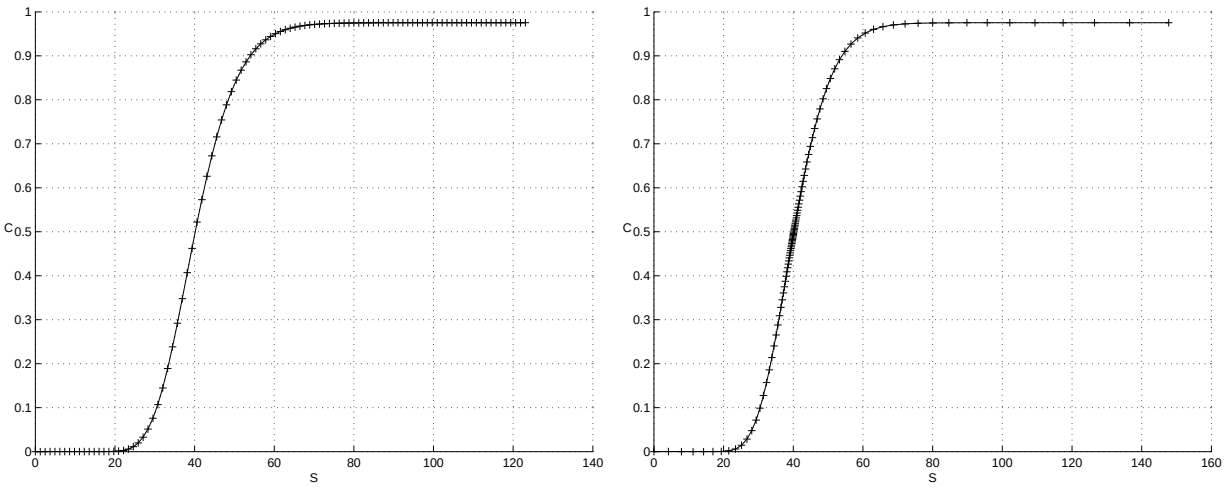

(a) Crank Nicolson, equidistant grid

(b) BDF4, stretched grid

Figure 7.3: Plots of solution C of a digital call option ($N = 100, M = 10$)

Grid	$\|C - C_{ex}\|_\infty$	Conv_∞	$\|\Delta - \Delta_{ex}\|_\infty$	Conv_∞	$\|\Gamma - \Gamma_{ex}\|_\infty$	Conv_∞
10×10	3.08×10^{-2}		2.22×10^{-2}		1.17×10^{-3}	
20×20	5.05×10^{-3}	6.09	3.47×10^{-3}	6.40	4.19×10^{-4}	2.80
40×40	3.34×10^{-4}	15.11	4.57×10^{-4}	7.60	8.02×10^{-5}	5.22
80×80	1.98×10^{-5}	16.92	3.54×10^{-5}	12.89	6.17×10^{-6}	13.00

Table 7.19: European digital call, E in the middle of two points $\mu = 1.875$

example, the error and the convergence of an asset-or-nothing call have been displayed. Furthermore, the results for the digital put and the asset-or-nothing put are shown in tables 7.21 and 7.22. From these tables, we observe that the convergence of Γ is less satisfactory (i.e. less than fourth order). One reason may be that the refinement is not on the position of the local minimum and maximum of Γ (see for example figure 3.13). Still the convergence is sufficient and the error in the hedge parameters is small with 20 to 40 grid points in space and time.

Grid	$\|C - C_{ex}\|_\infty$	Conv_∞	$\|\Delta - \Delta_{ex}\|_\infty$	Conv_∞	$\|\Gamma - \Gamma_{ex}\|_\infty$	Conv_∞
10×10	1.95		1.09		5.77×10^{-2}	
20×20	2.19×10^{-1}	8.91	1.47×10^{-1}	7.38	1.90×10^{-2}	3.04
40×40	1.45×10^{-2}	15.06	1.93×10^{-2}	7.61	3.34×10^{-3}	5.68
80×80	8.47×10^{-4}	17.17	1.49×10^{-3}	12.96	2.57×10^{-4}	13.02

Table 7.20: European asset-or-nothing call $\mu = 1.875$

Grid	$\|P - P_{ex}\|_\infty$	Conv_∞	$\|\Delta - \Delta_{ex}\|_\infty$	Conv_∞	$\|\Gamma - \Gamma_{ex}\|_\infty$	Conv_∞
10×10	3.08×10^{-2}		2.22×10^{-2}		1.17×10^{-3}	
20×20	5.05×10^{-3}	6.09	3.47×10^{-3}	6.40	4.19×10^{-4}	2.80
40×40	3.34×10^{-4}	15.11	4.57×10^{-4}	7.60	8.02×10^{-5}	5.22
80×80	1.98×10^{-5}	16.92	3.54×10^{-5}	12.89	6.17×10^{-6}	13.00

Table 7.21: European digital put $\mu = 1.875$

Grid	$\|P - P_{ex}\|_\infty$	Conv_∞	$\|\Delta - \Delta_{ex}\|_\infty$	Conv_∞	$\|\Gamma - \Gamma_{ex}\|_\infty$	Conv_∞
10×10	2.29		1.28		5.83×10^{-2}	
20×20	2.04×10^{-1}	11.21	1.38×10^{-1}	9.26	1.92×10^{-2}	3.04
40×40	1.40×10^{-2}	14.60	1.90×10^{-2}	7.28	3.32×10^{-3}	5.76
80×80	8.20×10^{-4}	17.06	1.51×10^{-3}	12.59	2.56×10^{-4}	13.00

Table 7.22: European asset-or-nothing put $\mu = 1.875$

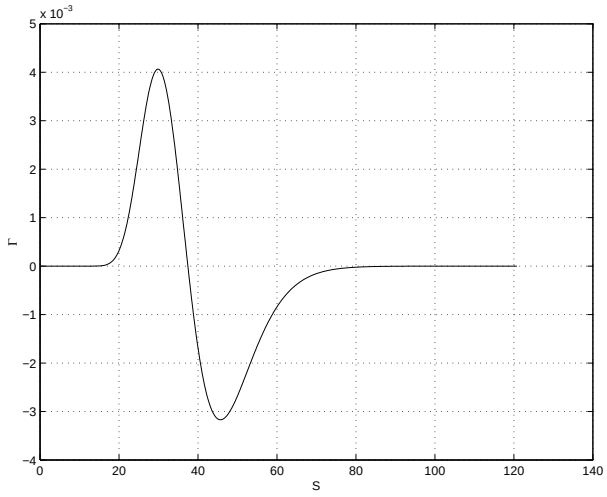

(a) Exact solution

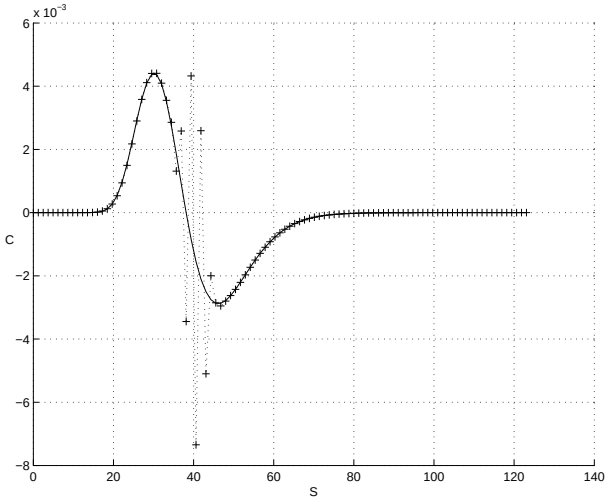

(b) Crank Nicolson, equidistant grid

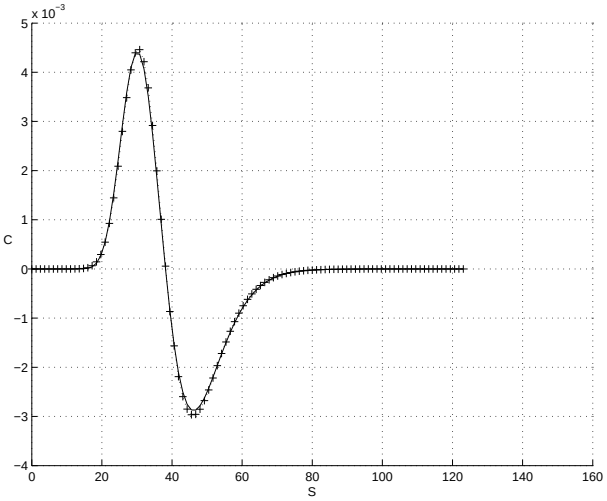

(c) Crank Nicolson after 2 backward Euler steps

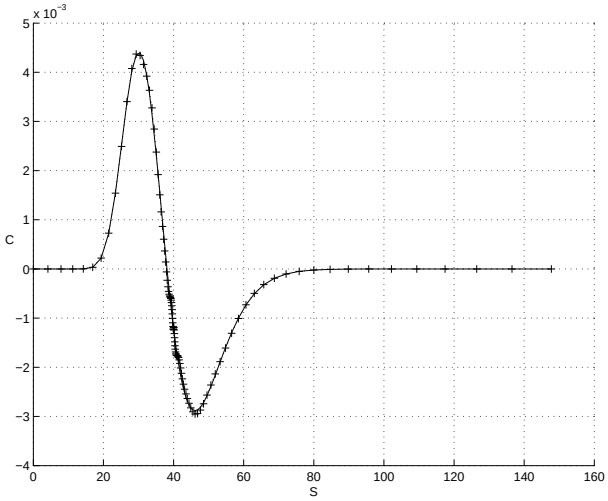

(d) BDF4, stretched grid

Figure 7.4: Plots of Γ of a digital call option ($N = 100, M = 10$)

7.3 Linear combinations

7.3.1 Spreads

When using the transformation and equation (6.4) to value spreads, some difficulties occur. First of all, if the spread is computed as a linear combination of two separate options, the grid stretching is not at the same position. That means that S coordinates of the two options are not identical. The two vectors have to be adjusted to each other. We can map the left option vector to the right option vector or vice-versa. For this purpose the Lagrange interpolation of fourth order will be used. The test for the bull spread with parameters as in section 3.3.5 is presented in table 7.23. It can be seen that the Lagrange

Grid	$\|V - V_{ex}\|_\infty$ adj. to E_1	Conv_∞	$\|V - V_{ex}\|_\infty$ adj. to E_2	Conv_∞
10×10	4.04×10^{-1}		3.93×10^{-1}	
20×20	1.16×10^{-1}	3.49	2.50×10^{-2}	15.69
40×40	3.26×10^{-3}	35.43	1.46×10^{-3}	17.17
80×80	2.62×10^{-4}	12.45	1.32×10^{-4}	11.02
160×160	1.71×10^{-5}	15.37	1.10×10^{-5}	12.02

Table 7.23: Solution of the Bull spread with $E_1 = 15$ and $E_2 = 25$ μE =constant, $R = 3$

interpolation gives irregular convergence. Still 40 grid points in space and time lead to a small error.

Also a butterfly spread is tested, where the two short position calls have an exercise price of $E_2 = \frac{1}{2}(E_1 + E_3)$. In table 7.24, the results have been displayed after the Lagrange interpolation. Again 40 points lead to satisfactory results.

Grid	$\|V - V_{ex}\|_\infty$ adj. to E_1	Conv_∞	$\|V - V_{ex}\|_\infty$ adj. to E_2	Conv_∞	$\|V - V_{ex}\|_\infty$ adj. to E_3	Conv_∞
10×10	2.62×10^{-1}		2.45×10^{-1}		2.50×10^{-1}	
20×20	6.38×10^{-2}	4.10	3.36×10^{-2}	7.30	6.20×10^{-2}	4.02
40×40	4.22×10^{-3}	15.11	2.76×10^{-3}	12.18	3.77×10^{-3}	16.45
80×80	2.49×10^{-4}	16.95	1.85×10^{-4}	14.88	2.82×10^{-4}	13.38
160×160	1.89×10^{-5}	13.22	1.16×10^{-5}	15.99	1.88×10^{-5}	14.97

Table 7.24: Solution of the Butterfly spread with $E_1 = 15$, $E_2 = 20$ and $E_3 = 25$ μE =constant, $R = 3$

One reason for the irregular convergence behaviour, is that the Lagrange interpolation maps regions with many grid points to regions with a few grid points. This influences the accuracy.

The double transformation, i.e. stretching around two grid points (4.43) would be a possibility for spreads. In that case the spread is handled in a single computation. However, the quality of these numerical results is not yet comparable to the results presented above.

7.4 Volatility search

Now we return to the first option, with parameters:

$$\begin{aligned} E &= 15 \\ r &= 4\ \% \\ \delta &= 2\ \% \\ T &= 0.5 \quad \text{half a year,} \end{aligned}$$

but we wish to compute the implied volatility. As described in section 6.6, the values of the option and asset price can be read from the newspaper. The volatility search methods from section 6.6 are applied with the fourth order Black-Scholes discretization on the stretched grid. Suppose, we have an option price of € 1.25, with asset price € 14.87. The asset price is not far from the exercise price. From table 7.9, it follows that 20 or 40 grid points should be enough to recover the option price. The volatility σ_{imp} should converge towards 0.3. The stopping criterion for the search methods is defined by a tolerance:

$$|C(\sigma_{imp}) - C_{market}| < \text{Tolerance}. \tag{7.1}$$

Both search methods are compared with a tolerance of 10^{-3} and with tolerance 10^{-5}. The convergence results are shown in tables 7.25 (bisection) and 7.26 (quadratic inverse interpolation).

	20×20 grid points		40×40 grid points	
Iteration number	Volatility	$\lvert C(\sigma) - C_{market}\rvert$	Volatility	$\lvert C(\sigma) - C_{market}\rvert$
1	0.5000	0.8284	0.5000	0.8182
2	0.2750	0.0985	0.2750	0.1024
3	0.3875	0.3661	0.3875	0.3591
10	0.2987	0.0004	0.3005	0.0023
16	0.2988	7.7×10^{-7}	0.2999	1.44×10^{-7}

Table 7.25: Volatility search with bisection and with (7.1)

We see that the inverse quadratic interpolation method converges very fast. Tolerance 10^{-3} is reached within 3 and tolerance 10^{-5} within 4 iterations. The bisection

	20×20 grid points		40×40 grid points	
Iteration number	Volatility	$\lvert C(\sigma) - C_{market} \rvert$	Volatility	$\lvert C(\sigma) - C_{market} \rvert$
1	0.4000	4.03×10^{-1}	0.4000	3.96×10^{-1}
2	0.3026	1.38×10^{-2}	0.3035	1.45×10^{-2}
3	0.2988	4.87×10^{-5}	0.2999	7.27×10^{-5}
4	0.2988	6.80×10^{-7}	0.2999	1.04×10^{-7}

Table 7.26: Volatility search with inverse quadratic interpolation (start values $\sigma_a = 0.2, \sigma_b = 0.4$ and $\sigma_c = 0.6$ and with (7.1)

method shows a slower convergence, as expected. It reaches tolerance 10^{-5} in 16 iterations. Furthermore, we observe that 20 grid points are not enough to recover the volatility accurately. The numerical convergence is towards $\sigma_{imp} = 0.2988$. With 40 points in space and time, $\sigma_{imp} = 0.3$ is found. The convergence of the search methods does not depend on the number of grid points in this experiment. The convergence of both methods is plotted in figures 7.5 and 7.6.

If we have S_0 not in the neighbourhood of E, the number of iterations increases. Suppose the option price is $C =$€ 4.05 and the asset price is $S_0 =$€ 19.23, the convergence results on a 40×40 stretched grid are presented in tables 7.27 and 7.28. Again the convergence of the quadratic inverse interpolation method is impressive.

Iteration number	Volatility	$\lvert C(\sigma) - C_{market} \rvert$
11	0.3001	1.41×10^{-4}
16	0.3000	4.37×10^{-6}

Table 7.27: Volatility search of the second test with bisection and with (7.1), 40×40 points.

Iteration number	Volatility	$\lvert C(\sigma) - C_{market} \rvert$
7	0.3000	1.84×10^{-5}
8	0.3000	2.48×10^{-9}

Table 7.28: Volatility search of the second test with inverse quadratic interpolation (start values $\sigma_a = 0.2, \sigma_b = 0.4$ and $\sigma_c = 0.6$ and with (7.1) 40×40 points.

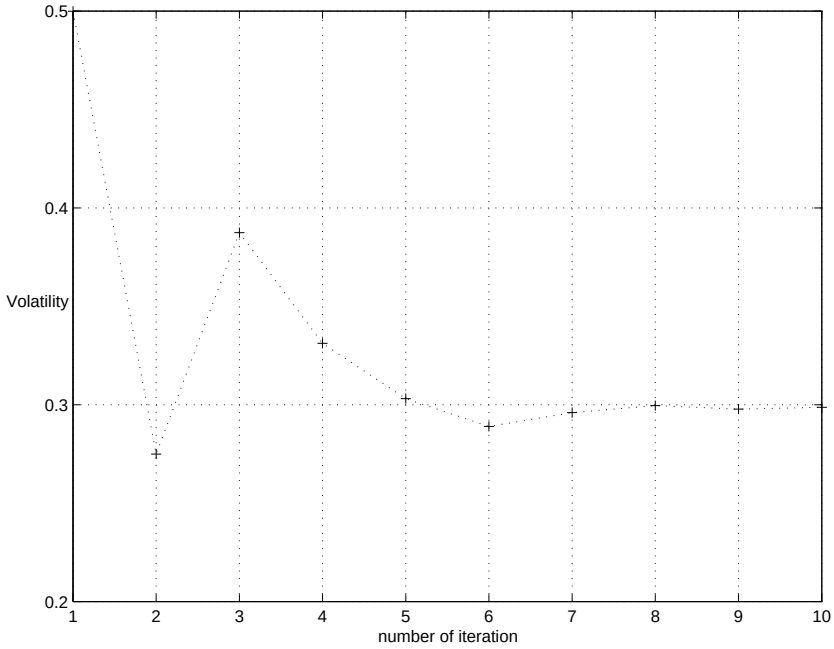

Figure 7.5: Convergence of the bisection method

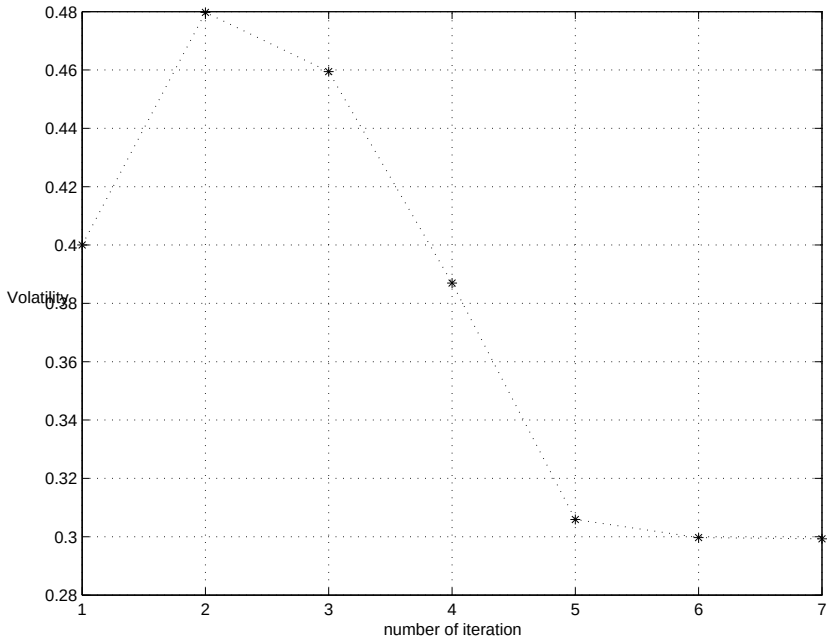

Figure 7.6: Convergence of the inverse quadratic interpolation method

Chapter 8

Conclusions

Option contracts can be valued by using a partial differential equation, the Black-Scholes equation. An exact solution for European style options is known. Numerical experiments are necessary to determine the value of American style options and for many exotic options. The calculation time must be minimized as well as the error. In this thesis we have solved the Black-Scholes equation in as few grid points as possible. We have valued only options for which an analytic solution is known. Furthermore we are interested in the accuracy of the hedge parameters. An overall fourth order accurate space and time discretization is proposed in this thesis, using grid stretching by means of an analytical coordinate transformation. Due to the final conditions, the equidistant grid discretization does not have the property of fourth order convergence. With the proper choices of grid, stretching parameter μ and maximal grid size, fourth order accuracy can be achieved as well as a very small error in the option value and in the hedge parameters with only 20-40 grid points. The relation found by experiments for μ is defined by $\mu E =$ constant. For our reference option, the constant value 75 is very satisfactory.

Digital options are exotic options with a discontinuous final condition. Whereas Crank-Nicolson shows oscillations in hedge parameter Γ, BDF4 is accurate in all hedge parameters. With the transformed fourth order accurate scheme, the coordinate $S = E$ must be exactly between two grid points for fourth order convergence. Then, also for digital options, a small error is obtained with a few grid points.

The implied volatility, which is important information to value an option with given option price and asset price, can be found in less than 10 iterations by applying the inverse quadratic interpolation. The error decreases almost quadratically for our reference option.

Summarizing, the answers to the questions posed in the introduction are:

- For our reference problem, only 20-40 space- and time-steps are sufficient to get an accuracy of one cent (€ 0.01) with the use of grid stretching and highly accurate discretization schemes. With E large, the number of steps must be increased, although, one cent is very small compared to large values of E.

- The scheme also works well for exotic options, like digital options, asset or nothing options and combinations of options.
- The volatility can be calculated in less than ten iteration steps.

The scheme proposed can be generalized to higher dimensional problems , for example options on more assets. Time stretching may be necessary for discontinuities in the boundary conditions, for example with discrete dividends. The American option can be performed with a double stretching, both in space as in time.

Chapter 9

Appendix 1: Exact solutions of the Greeks

General notations

$$d_1(S,t) = \frac{\ln S - \ln E + \left(r - \delta + \frac{1}{2}\sigma^2\right)(T-t)}{\sigma\sqrt{T-t}} \tag{9.1}$$

$$d_2(S,t) = d_1(S,t) - \sigma\sqrt{T-t} = \frac{\ln S - \ln E + \left(r - \delta - \frac{1}{2}\sigma^2\right)(T-t)}{\sigma\sqrt{T-t}} \tag{9.2}$$

$$N(x) = \frac{1}{\sqrt{2\pi}} \int_{-\infty}^{x} e^{-\frac{1}{2}y^2} dy \tag{9.3}$$

$$N'(x) = \frac{dN}{dx} = \frac{1}{\sqrt{2\pi}} e^{-\frac{1}{2}x^2} \tag{9.4}$$

European call

$$C(S,t) = Se^{-\delta(T-t)}N(d_1) - Ee^{-r(T-t)}N(d_2) \tag{9.5}$$

$$\Delta(S,t) = e^{-\delta(T-t)}N(d_1) \tag{9.6}$$

$$\Gamma(S,t) = e^{-\delta(T-t)}\frac{N'(d_1)}{\sigma S\sqrt{T-t}} \tag{9.7}$$

$$\Theta(S,t) = -\frac{\sigma S N'(d_1)}{2\sqrt{T-t}} - rEe^{-r(T-t)}N(d_2) \tag{9.8}$$

$$\mathcal{V}(S,t) = SN'(d_1)\sqrt{T-t} \tag{9.9}$$

$$\rho(S,t) = E\,(T-t)\,e^{-r(T-t)}N(d_2) \tag{9.10}$$

European put

$$P(S,t) = Ee^{-r(T-t)}N(-d_2) - Se^{-\delta(T-t)}N(-d_1) \tag{9.11}$$

$$\Delta(S,t) = e^{-\delta(T-t)}\left(N(d_1) - 1\right) \tag{9.12}$$

$$\Gamma(S,t) = e^{-\delta(T-t)}\frac{N'(d_1)}{\sigma S\sqrt{T-t}} \tag{9.13}$$

European digital call

$$C(S,t) = Qe^{-r(T-t)}N(d_2) \tag{9.14}$$

$$\Delta(S,t) = Qe^{-r(T-t)}\frac{N'(d_2)}{\sigma S\sqrt{T-t}} \tag{9.15}$$

$$\Gamma(S,t) = -Qe^{-r(T-t)}\left(\frac{N'(d_2)}{\sigma S^2\sqrt{T-t}} + \frac{d_2N'(d_2)}{\sigma^2S^2(T-t)}\right) \tag{9.16}$$

European asset or nothing call

$$C(S,t) = Se^{-\delta(T-t)}N(d_1) \tag{9.17}$$

$$\Delta(S,t) = e^{-\delta(T-t)}\left(N(d_1) + \frac{N'(d_1)}{\sigma\sqrt{T-t}}\right) \tag{9.18}$$

$$\Gamma(S,t) = \frac{e^{-\delta(T-t)}}{\sigma S\sqrt{T-t}}\left(N'(d_1) - \frac{d_1N'(d_1)}{\sigma\sqrt{T-t}}\right) \tag{9.19}$$

$$\tag{9.20}$$

European digital put

$$P(S,t) = Qe^{-r(T-t)}N(-d_2) \tag{9.21}$$

$$\Delta(S,t) = -Qe^{-r(T-t)}\frac{N'(d_2)}{\sigma S\sqrt{T-t}} \tag{9.22}$$

$$\Gamma(S,t) = Qe^{-r(T-t)}\left(\frac{N'(d_2)}{\sigma S^2\sqrt{T-t}} + \frac{d_2N'(d_2)}{\sigma^2S^2(T-t)}\right) \tag{9.23}$$

European asset or nothing put

$$P(S,t) = Se^{-\delta(T-t)}N(-d_1) \tag{9.24}$$

$$\Delta(S,t) = e^{-\delta(T-t)}\left(N(-d_1) - \frac{N'(d_1)}{\sigma\sqrt{T-t}}\right) \tag{9.25}$$

$$\Gamma(S,t) = \frac{e^{-\delta(T-t)}}{\sigma S\sqrt{T-t}}\left(-N'(d_1) + \frac{d_1N'(d_1)}{\sigma\sqrt{T-t}}\right) \tag{9.26}$$

$$\tag{9.27}$$

Bibliography

[1] Björk, T., *Arbitrage theory in continuous time,* Oxford University Press, Oxford, 1998.

[2] Boyce, W.E., Diprima, R.C., *Elementary differential equations and boundary value problems,* Wiley Publ., New York, 1997.

[3] Brzezniak, Z, Zastawniak, T, *Basic stochastic processes,* Springer Verlag, Heidelberg, 1998.

[4] Burden, R.L., Douglas Faires, J., *Numerical analysis,* Brooks/Cole, Grove, 7th ed., 2001.

[5] Cartwright, J.J.E., Piro, O. The dynamics of Runge-Kutta methods. *Int. J. Bifurcation Chaos,* 2:427-449, 1992.

[6] Clarke, N. Parrot, K., Multigrid for American option pricing with stochastic volatility, *Appl. math. finance,* 6:177-179, 1999.

[7] Hairer, E., Nörsett, Wanner, K., *Solving ordinary differential equations. Vol. 1. Non-stiff problems,* Springer Verlag, Heidelberg, 1996.

[8] Hairer, E., Wanner. K., *Solving ordinary differential equations. Vol. 2. Stiff and differential-algebraic problems,* Springer Verlag, Heidelberg, 1996.

[9] Heath, M. Th., *Scientific computing,* McGraw Hill, New York, 2nd edition, 2002

[10] Hull, J.C., *Options, futures and other derivatives,* Prentice-Hall Int. Inc, London, 1989.

[11] Kangro, R, Nicolaides, R. Far field boundary conditions for Black-Scholes equations, *SIAM J. Numerical Analysis,* 38(4): 1357-1368, 2000.

[12] Kwok, Y.K., *Mathematical models of financial derivatives.* Springer Verlag, Heidelberg, 1998.

[13] Lay, D.C., *Linear Algebra and its applications,* Addison-Wesley, New York, 2nd ed. 2000.

[14] Pooley, D., Numerical methods for Nonlinear Equations in Option Pricing, Ph.D. Thesis, University of Waterloo, Waterloo (Canada), 2003.

[15] Rannacher, R., Finite element solution of diffusion equation with irregular data, *Num. Math.,* 43: 309-327, 1984.

[16] Segal, A., *Numerieke methoden voor partiële differentiaalvergelijkingen,* VSSD Delft, Delft, 1993.

[17] Strauss, W.A. *Partial differential equations, an introduction,* Wiley Publ., Singapore, 1992.

[18] Wesseling, P., *Principles of computational fluid dynamics,* Springer Verlag, Berlin, 2001.

[19] Wilmott, P, Howison, S, Dewynne, J., *The mathematics of financial derivatives,* Cambridge University Press, Cambridge, 1997.